THE EFFECTS OF SOMATOSENSORY AFFERENCE ON CORTICOSPINAL EXCITABILITY IN UNINJURED AND SPINAL CORD INJURED INDIVIDUALS

BY AARON Z. BAILEY B.Sc.

A Thesis Submitted to the School of Graduate Studies in Partial Fulfillment of the Requirements for the Degree Masters of Science

McMaster University

DESCRIPTIVE NOTE

McMaster University MASTER OF SCIENCE (2015) Hamilton, Ontario (Kinesiology)

TITLE: The Effects of Somatosensory Afference on Corticospinal Excitability in Uninjured and Spinal Cord Injured Individuals

AUTHOR: Aaron Z. Bailey (McMaster University)

SUPERVISOR: Professor A.J. Nelson

NUMBER OF PAGES: x, 87

ABSTRACT

Primary somatosensory cortex (SI) is an important cortical structure involved in receiving and relaying sensory inputs to condition primary motor cortex (M1). The functional interaction between SI and M1 is important for motor control by providing surround inhibition, which is the inhibition of muscles not involved in the movement and in learning new motor skills. This interconnection is known as short-latency afferent inhibition (SAI) and may be probed using Transcranial magnetic stimulation and peripheral nerve stimulation. SAI is dependent on the afferent volley as increasing the nerve stimulation intensity increases the depth of SAI. Individuals with spinal cord injury show reductions in SAI evoked in lower limb and this may be a contributing factor to the impairments in motor control seen within this population. SAI has yet to be investigated in the upper limb in individuals with chronic cervical SCI and this thesis examines these alterations. Two experiments were performed examining M1 excitability (motor evoked potentials), SI excitability (somatosensory evoked potentials) and the interconnection between SI and M1 (SAI). The first Experiment investigated alterations in these measures in individuals with SCI while the second Experiment investigated these measures as a function of the afferent volley. The collective results from Experiment 1 indicate that motor evoked potentials and SAI are reduced but somatosensory evoked potentials are similar to controls. Further data from Experiment 2 indicate that SAI and SEPs increase as a function of the afferent volley and indicate that alterations seen in individuals with SCI may be due to cortical plasticity in the synapses from SI to M1 or within M1. The novel findings of this thesis have indicated aberrant cortical circuits in individuals with

SCI and have indicated potential synapses that may be targets for TMS plasticity protocols to alter and restore function to these circuits.

ACKNOWLEDGEMENTS

I would like to first and foremost thank my supervisor Dr. Aimee Nelson. Your guidance and advice over the past two years has taught me the dedication, diligence and effort required to be successful in not only academia but also in life. I will always view these past two years as a time of personal growth in all aspects of my life. All of the lessons I have learned from you will be taken forward in all my future endeavors allowing me to continue to be successful, and for this I thank you.

I would also like to thank my committee members, Dr. Audrey Hicks and Dr. Kathleen Martin Ginis, for their assistance in the completion of my Thesis. Your advice and guidance proved to greatly improve the quality of my research.

To my fellow colleagues of the Kinesiology department, the atmosphere you all create within the basement hallways of Ivor Wynne Center is an excellent support network that vastly improves the enjoyment of coming into school every day.

I would like to thank all my fellow lab-mates, or Nelsons Neuron; Peter Mi, Tanner MacKenzie, Mike Asmussen, Christy Jones, Phil Tsang and Tea Lulic. I will remember all the great times we all had inside and outside the lab. You have made this journey much more enojoyable.

Last I would like to thank my family and friends for their continual support during the past two years. It was a hard road but you helped me make it to the end!

DECLARATION OF ACADEMIC ACHIEVEMENT

The entirety of this thesis has been written, and all experiments were conceived and performed, by myself. Dr. Aimee J. Nelson aided conception of studies, and my fellow lab mates, Mike Asmussen, Peter Mi, Tanner MacKenzie, Christy Jones and Phil Tsang, aided the collection of data.

Table of Contents

List of Figures

List of Tables

List of Abbreviations

APB	Abductor Pollicis Brevis
AMT	Active Motor Threshold
ANOVA	Analysis of Variance
CS	Conditioning Stimulus
CNS	Central Nervous System
CSN	Corticospinal Neuron
D-wave	Direct Wave
EMG	Electromyography
FCR	Flexor Carpi Radialis
ISI	Interstimulus Interval
I-wave	Indirect Wave
PPR	Paired-pulse ratio
M1	Primary Motor Cortex
MEP	Motor Evoked Potential
MSO	Maximum Stimulator Output
PC	Pyramidal Cells
PV	Parvalbumin
RMT	Resting Motor Threshold
SAI	Short-latency afferent inhibition
SCI	Spinal Cord Injury
SEP	Somatosensory evoked potentials
SNAP	Sensory nerve action potentials
SI	Primary Somatosensory Cortex
TES	Transcranial Electrical Stimulation
TMS	Transcranial Magnetic Stimulation
TRN	Thalamo reticular nucleus
TS	Test Stimulus
μV	Microvolts
VPL	Ventro-posterior lateral nucleus

Chapter 1: Goals of Thesis

1.1 Overview of Thesis

The goal of this Master's thesis was to 1) investigate the effects of a somatosensory afferent input on the excitability of the motor cortex and how this may have changed in a group with a spinal cord injury (SCI) and 2) investigate the effects of the magnitude of the afferent input on neural activity within primary somatosensory and motor cortices (SI, M1). At a distinct latency, afferent input has a strong inhibitory effect on the motor cortex, a circuitry termed short-latency afferent inhibition (SAI) [1]. This inhibitory circuit is thought to play an important role in gating cortical excitability during movement by inhibiting non-moving, uninvolved muscles, a concept known as surround inhibition [2,3]. SAI is altered in many movement disorders such as focal hand dystonia, [4,5] Parkinson's disease,[6] and following stroke [7,8]. SCI leads to a decrease in somatosensory afferent input to the cortex,[9] a decrease in corticospinal output from the cortex,[10] cortical reorganization within SI [11,12] and M1[11,13]and these alterations may lead to aberrations in cortical function within M1, SI and the communication between the two. To date no research has been provided on the sensorimotor integration in upper limbs of individuals with cervical spinal cord injury. Further, altering the intensity of the somatosensory afferent volley has been shown to change these cortical responses in that somatosensory evoked potentials (SEPs), paired pulse ratio (PPR) and SAI all increase with an increase in the nerve stimulus intensity. However, it is not known how these measures respond to an increase or decrease in the afferent volley, something likely to be present in an individual with SCI and this information would

greatly assist in the interpretation of alterations in sensorimotor function observed in individuals with SCI.

1.2 Summary of Experiments

Experiment 1 examined measures of M1 function through motor evoked potentials (MEPs) and thresholds, SI function through sensory nerve action potentials (SNAPs), SEPs and sensorimotor connectivity through SAI in individuals with spinal cord injury (SCI) compared to uninjured controls. TMS was performed over flexor carpi radialis (FCR) and MN stimulation was used to evoke SNAPs, SEPs and SAI (ISIs of 15, 20 and 25 ms) in both resting and active states. Eight individuals with SCI were studied bilaterally (12 limbs total) across three sessions and compared to thirteen age-matched controls. Results indicate that SNAPs SAI, and MEPs are reduced in SCI but SEPs are not. Therefore, we conclude that reduced SAI in SCI may be due to decreased projections from SI to M1 or in the intrinsic motor circuitry mediating SAI. These data provide a new avenue of research aimed at therapeutic approaches to alter SAI and restore upper limb function in individuals with SCI.

The objective of Experiment 2 was to further investigate the effect of increasing stimulus intensity, based on % $SNAP_{max}$ on measures of SEPs, PPR and SAI. The second objective was to investigate the relationship between SEPs, PPR and SAI. Twenty-three right-handed individuals were studied. The median nerve was stimulated at the wrist using stimulus intensities of ~ 25%, 50%, and 75% $SNAP_{max}$ and 1.2 x and 2.4 x MT. SEPs, PPR and SAI increase from 20% to ~ 50 % $SNAP_{max}$ and do not increase significantly beyond this intensity (i.e. saturation point). Further, correlations between

SAI and SEPs as well as SAI and PPR were significant. Data reveal similarities in the stimulus-response profiles of SEPs, PPR and SAI and correlations provide further support for the relationship between excitation within primary somatosensory cortex and inhibition within primary motor cortex. These data can be used as a guideline for choosing appropriate intensities for intervention type studies that aim to reveal increases and/or decreases in one or more of these measures.

1.3 Significance of Work

The characterization of MEPs, SNAPs, SEPs and SAI in an SCI population is an important step in determining the cortical areas that may serve as targets for plasticity-inducing protocols that aim to change the effectiveness of these circuits. The circuits SAI and LAI have been chosen because they have been implicated in the sensorimotor integration of human movement by providing the concept of surround inhibition. Surround inhibition being the inhibition of corticospinal output to muscles not involved in movement, i.e., digit 5 is showing inhibition when digit 2 is moving. The SCI population, who may have alterations to sensory perception as well as decreases in the amount of afferent information that arrives at the cortex, are good candidates to show changes to these neural circuits resulting in aberrant sensorimotor integration.[9] In this thesis the upper limb has been chosen to study because tetraplegics with incomplete spinal cord injury rely on their upper limbs for a majority of their activities of daily living (ADL's).[14] Small improvements in function within the upper limb can have a large impact on the ability to perform ADL's and it has been shown that regaining upper limb function is a top priority to those with a cervical spinal cord injury.[14]

Chapter 2: Literature Review

2.1 Relevant Anatomy

2.1.1 Anatomy of the Spinal Cord

The spinal cord is a critical structure in the transmission of information to and from the cortex. The spinal cord is divided into central gray matter and peripheral white matter.[15] The gray matter is composed mainly of neuron cell bodies. It is divided in the midline by a dorsal and ventral gray commissure and from here can be further divided into a posterior (dorsal) horn, an anterior (ventral) horn and a lateral horn. [16,17] The gray matter of the dorsal horn contains neurons that pertain to inputs from sensory afferents. The gray matter of the ventral horn is primarily made of alpha motoneurons concerned with innervating skeletal muscle.[16,17] The lateral horn can only be found in the thoracic region of the spinal cord and is primarily made of preganglionic sympathetic neurons. The white matter is divided into three areas (funiculi), the posterior (dorsal), lateral, and anterior (ventral) funiculi. Each of the funiculi contain heavily myelinated nerve fiber bundles that travel together and serve the same function.[16] These bundles are referred to as fasciculi and the dorsal funiculus is divided into two main fasciculi named gracilis and cutaneous. The nerve fibers within the dorsal funiculi are ascending and contain sensory information relating to proprioception and discriminative touch.[16] Specifically nerve axons that are added before the sixth thoracic level (lower limb) are added to the gracilis fasciculus and those that are added after the sixth thoracic level (upper limb) are added to the cutaneous fasciculus. Ascending fascicles in the ventral funiculi are associated with light touch and those in the lateral funiculi are associated with pain and temperature discrimination.[18]

2.1.2 Anatomy of the Motor Cortex

The primary motor cortex (M1) is the primary source for efferent motor commands to produce voluntary movement. M1 is located just anterior to the central sulcus and sends projections to the spinal cord from mainly corticospinal (CST) neurons embedded in laver V. There exist two types of CST neurons, the first terminating onto interneurons in the intermediate zone of the spinal cord. The second terminate onto motoneurons in the ventral horn of the spinal cord and are termed corticomotoneuronal (CM).[19] Through studies of rhesus monkeys the CM have been found only in the caudal region of M1 meaning a certain area of M1 has direct control over motor output.[20] Additionally, studies that observe the effects of local lesions have created motor maps of M1 and have observed an orderly arrangement of body parts from foot (medial) to hands and face (lateral).[21] However, the somatotopic map is not clearly defined as a collection of separate areas for each muscle.[22] Rather the muscle representations are broadly distributed within M1 and a single muscle can have multiple representations within the cortex, and can even overlap with other muscles.[21,22] When these multiple representations are averaged a clear medial to lateral organization of the proximal to distal muscles is seen.[22,23]

2.1.3 Anatomy of the Thalamus

The thalamus makes up the dorsal portion of the diencephalon and is a crucial link between the sensory afferent pathway and the somatosensory cortex (SI). The thalamus is divided into four areas named; anterior, medial, ventrolateral and posterior.[22,24]

Specifically three main nuclei within the posterior nuclei have been labeled as important in relaying sensory information; the ventroposterior nucleus (VP), ventroposterior inferior nucleus (VPI) and the ventroposterior superior nucleus (VPS).[25] The VP nucleus can be divided into two areas, the VP medial (VPM) and the VP lateral (VPL). The VPM is responsible for afferent projections from the face and the VPL is responsible for afferent projections from the upper and lower limbs.[18] While the VPI responds to cutaneous and painful stimuli[26] and the VPS responds to proprioceptive information from muscle spindles.[3,27,28] All areas of the thalamus relay information to the somatosensory cortex but is regulated by the thalamic reticular nucleus (TRN). Depending on the type of information coming and from where the TRN acts like a sieve and controls the messages that reach the cortex. The TRN recognizes inputs from the thalamus as either first order (cells in thalamus that receive input form ascending afferent fibers) or higher order (cells in the thalamus that receive input from the cortex). In the somatosensory system both orders are received by the same TRN cells when relay the first order information to the anterior area of the SI while higher order information is relayed to the lateral area of SI.[29]

2.1.4 Anatomy of the Somatosensory Cortex

The somatosensory cortex (SI) is located just posterior to the central sulcus and is comprised of 4 areas named Brodmann areas 3b, 3a, 2, and 1. Each area pertains to a different sensory representation of the body.[30] Brodmann area 3b is important in integrating cutaneous information as this area responds best to cutaneous stimuli. Area 3b is also found to be the most densely myelinated Brodmann area.[31] Area 3a receives

projections from VPS in the thalamus[31,32] regarding muscle spindle afferent information,[31] as well as information from area 3b regarding cutaneous information.[33-35] Area 1 receives a modulating input from VP as well as an excitatory input from area 3b[34,35] regarding cutaneous information.[35-37] Area 2 combines both tactile information from areas 1 and 3b[33,35,36] and proprioceptive sensory information from VPS in the thalamus[38] to mediate tactile information of objects.[17] Each area has a unique somatotopic map of the body with area 3b representing the classic map of SI.[17,39-41] Somatotopic organization begins at the level of the spinal cord as afferents are added in a medial to lateral fashion as you ascend the spinal cord.[17] Brain imaging of anterior parietal cortex during sensory driven activation from contralateral body regions show a medial to lateral somatotopy from foot-hand-face.[42] The cortical magnification factor for a particular body part within the sensory cortex is determined by its relative importance in our sensory perception.[17]

2.2 Afferent Stimulation

2.2.1 Transmission of Afferent Input to SI (SNAPs)

Within the skin four cutaneous mechanoreceptors are responsible for responding to an external stimulus. These cutaneous mechanoreceptors belong to two groups, the first are classified as rapidly adapting and the second are classified as slow adapting. Rapidly adapting receptors only respond to rapid indentation of the skin and include Merkel cells, and Pacinian afferents. Slowly adapting receptors respond to a sustained skin deformation and include Ruffini endings and Meissner corpuscles.[42] When a tactile stimulus

activates these mechanoreceptors action potentials in somatosensory afferent fibers are transmitted along the axons and collect at the dorsal root ganglion just prior to entering the spinal cord.[17,42] The amount of activation of peripheral nerves can be quantified by placing surface electrodes overtop of the nerve stimulated at a proximal location to the stimulation site. These recordings are known as sensory nerve action potentials (SNAPs) and increases in the amplitude reflect increases in the fibers recruited. If a mixed nerve (i.e., median nerve) is stimulated the recording from this nerve is likely to be a mix of afferent fibers and antidromic recruitment of efferent fibers. The axons recruited travel into the spinal cord via the dorsal horn and either synapse in the grey matter to form local circuits, or ascend via dorsal columns, specifically, the cuneate fascicle, to the cuneate nucleus located at the medulla. These local circuits within the grey matter form reflex loops, while the ascending pathways refer the afferent information to the cortex. At the medulla information travels through the sensory decussation to the contralateral side of the brain and continues through the medial lemniscuses to synapse with the VP nucleus within the thalamus.[17,42] The VP nucleus projects laterally to SI synapsing with spiny stellate neurons in layers IV and VI which then project to the apical dendrites of the pyramidal neurons in layer III.[22,23]

2.2.2 Somatosensory Evoked Potentials

Somatosensory evoked potentials (SEPs) are measurements of cortical activity in response to a somatosensory cue, typically from electrical nerve stimulation.[43] Measurements are made by placing electroencephalography (EEG) electrodes over various parts of the brain based on the 10-20-measurement system.[43] The resulting

waveform has many positive (P) and negative (N) inflections at different latency's, which pertain to different parts of the ascending sensory tract. When stimulating the median nerve at the wrist, an N10 inflection represents the afferent path travelling through the brachial plexus, and the N12/13 represent the pre-synaptic spinal afferent volley and lower medullary activity.[44] The sensory information reaching SI causes a synaptic excitation of the pyramidal neurons generating an excitatory post-synaptic potential (EPSP), which travels to other pyramidal neurons in the cortex.[24] This is characterized by a negative inflection at latency of 20ms and is referred to as N20.[44] The latency of the N20 is dependent on the participant's age, sex and body size. As a child grows the latency of the N20 increases and begins to plateau at around 17 years of age. From 18-94 years of age the latency continues to grow but at a slower rate, and males on average have a longer latency when compared to females.[44] When active EEG electrodes are placed over C3, P3 and Cz, based on the 10-20-measurement system, N20's are most consistent.[45] SEP amplitudes grow in response to greater nerve stimulation intensities, greater afferent drive, as shown by an increase to the N20 component[20]. However, this increase is sigmoid and plateaus at a stimulus intensity equal to 50% of the maximum afferent volley.[46]

2.2.3 Paired-Pulse Somatosensory Evoked Potentials

Paired-pulse SEP's have been used widely in previously literature to explore the excitability of SI. By electrically stimulating a peripheral nerve twice in close succession two responses are evoked in SI. The second stimulus is significantly suppressed when the two responses are separated by short ISI's, approximately 30 ms, and approaches baseline

at longer ISI's, ~200 ms.[20,47] The degree suppression in the second stimulation depends on the interstimulus intervals between the two stimulations, as well as the intensity of the first stimulation.[20,47] The N20 component and the N20-P25 component of the second SEP have been shown to decrease (i.e., more inhibition), with an increase in nerve stimulation intensity. However the N20-P25 component is affected to a greater extent than the N20. This could be because the N20 is generated by Brodmann area 3b and receives heavy projection from VPL nucleus of the thalamus where the N20-P25 is likely generated by Brodmann area 1 which is weakly innervated by small diameter fibers from the thalamus, and is heavily connected with Brodmann area 3b. [20,48] The exact mechanism to which paired pulse suppression happens are not fully understood though animal studies provide evidence to suggest a suppression in the thalamocortical[49] and intracortical synapses[50] as well as a thalamic afferents activating a feed forward inhibition driven by GABAergic interneurons.[51]

2.2.4 SI-M1 Connectivity

Somatosensory cortex has widespread connections to several other cortical areas. Studies performed in monkeys examined the effects of SI lesions on other cortical areas.[52,53] After a lesion was applied to majority of the somatosensory cortex degeneration was observed in four other cortical areas, precentral gyrus, fronto-parietal operculum, superior parietal lobule and the marginal gyrus on the medial surface of the hemisphere. The area of degeneration in the precentral gyrus conforms closely to the motor cortex (Area 4) but does not extent to the premotor area or supplementary motor area (Area 6).[52] When the lesion to SI is limited to certain areas patterns of degeneration are seen. When lesions

area applied to the SI representations for hind limbs and forelimbs degeneration is seen in the same representations within M1.[52] However when the SI representation for the trunk is lesioned the degeneration of neurons in M1 is not only in the trunk area but also extend towards the head and tail areas. In addition when lesions are applied to specific Brodmann areas within SI degeneration travels to the other areas within SI as well. A lesion in area 3b travels to areas 3a, 1, 2, 5 and 4; this is consistent for all areas of SI.[52,53] However, a study by Vogt and Pandya (1978), used specific small lesions and found no direct projections from area 3b to area 4. Instead they found dense connections to area 1. From area 1 they found dense connections to area 4. This suggests that lesions to area 3b affect area 4 through the intermediate area 1.[48] In addition, the only evidence for degeneration to SI from other areas in the brain come from lesions to M1.[52] It is clear that there are extensive interconnections between SI and M1, extensive enough to cause atrophy if either of their input is diminished.[52] The interconnectivity between these two areas is thought to be responsible for learning new tasks. When monkeys are learning a novel task and SI is lesioned prior to training the task is not learned, but when SI is lesioned after training the task is learned.[54]

2.3 Transcranial Magnetic Stimulation

2.3.1 Introduction

Transcranial Magnetic Stimulation (TMS) is a non-invasive approach to investigate the neurophysiology of the central and peripheral nervous system in humans[55]. TMS is based on the principal of electromagnetic induction of a current in the brain with the ability to excite neurons.

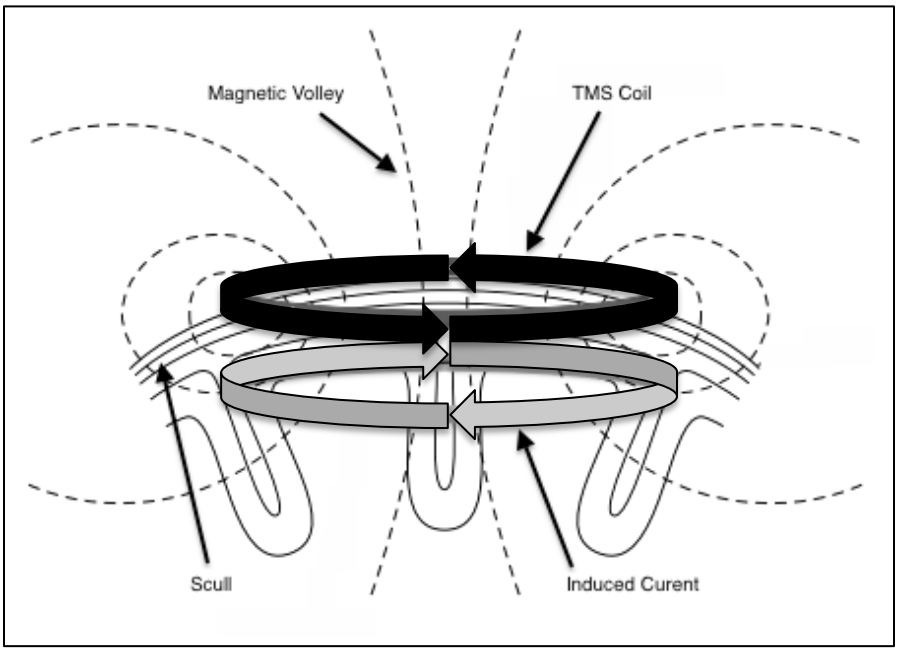

Fig 1. Illustration of the induced current within the brain caused by TMS. Modified from; Hallett et al., 2007

The magnetic field can reach 2 Tesla and lasts for around 100 microseconds.[56] According to Faraday's law the intensity of the magnetic field induced from TMS is proportional to the rate of change of current within the coil.[57] Understanding the effect TMS has on the brain has mainly come from activating the motor cortex in comparison to transcranial electrical stimulation (TES). Following stimulation of the motor cortex with TES, regardless of intensity, recordings of the corticospinal tract show an initial direct wave (D-Wave) followed by several indirect waves (I-waves) separated by ~1.5ms each.[56] These correlate to direct activation of the corticospinal neurons in motor cortex and a transsynaptic activation of the corticospinal neurons through interneurons, respectively.[30] In comparison TMS preferentially recruits I-waves at lower intensities, and D-waves at high intensities or lateral-medial coil orientation.[30,55] The affinity TMS shows toward generation of I-waves suggests an activation of superficial pyramidal

interneurons, which have excitatory synapses with corticospinal neurons.[30,55] The volleys travel down the spinal cord and summate at the spinal alpha motor neurons as an excitatory post synaptic potential (EPSP). If this EPSP is sufficient to depolarize the spinal motoneuron pool an action potential is generated to cause a motor response in the represented muscle.[58] These responses may be measured by surface electromyography (EMG) and can be used as a measure to assess nervous propagation and cortical/corticospinal excitability.[59,60]

2.3.2 Motor Evoked Potentials

Motor evoked potentials (MEPs) are the resulting muscle responses to a TMS pulse that is sufficient in intensity to depolarize the spinal motoneuron pool.[58] Muscles of the upper limb are significantly more accessible to TMS because they are superficial under the scalp where they lower limb is buried in the interhemispheric fissure.[55] The cortical projections to muscles reflects the complexity of movement those muscles are involved in.[61] Also distal muscles tend to have larger MEPs than proximal muscles, meaning they are more excitable by TMS. This could be because of increased cortical projections due to dexterity needed in the muscles of the hand for example, but could also be because of a disynaptic pathway to these muscles.[61] Flexor carpi radialis (FCR) is the muscle to be investigated in this thesis. MEPs are recorded in FCR using surface EMG electrodes in response to TMS. Since focality of surface electrodes is not fine enough to distinguish FCR from other muscles of the forearm MEP traces can be polyphasic, and if placed in belly-belly MEPs are quite small due to the differential amplifier subtracting two traces. If electrodes are placed in a belly-tendon fashion the differential amplifier only sees one

MEP and does not subtract anything from it, resulting in a larger more biphasic waveform. However since polyphasic responses still exist calculation of the area under the curve rather than peak-to-peak amplitude to quantify the muscle response must be used. The MEP size is a reflection of the excitability at both the cortical and spinal level.

2.3.3 Motor Threshold

Motor threshold (MT) is measure of corticospinal excitability, the faster a muscle responds to TMS and the larger the response the more excitable that muscle is.[62] Muscle responses across participants occur at different TMS intensities and the threshold for muscle responses is therefore different among individuals. It is important to therefore have a method to standardize the TMS intensity used in participants. MT allows the stimulator to be set at an intensity that is relative to participant's sensitivity to TMS. MT can be calculated in both the active and resting state. Resting motor threshold (RMT) is defined as the minimum stimulator intensity needed to elicit a motor response of 50 microvolts in at least 5 out of 10 trials.[63] Active motor threshold (AMT) is defined as the minimum stimulator intensity needed to elicit a motor response of 200 microvolts in at least 5 out of 10 trials, while participants hold a slight tonic contraction of the target muscle.[63,64] AMT is generally lower than RMT because corticospinal axons and tracts are already being pre-activated and are more sensitive to the TMS pulse.[62] Pharmacological evidence suggests that RMT indicates the membrane threshold[65] where AMT indicates the number of axons that are close to firing threshold.[62] Much care is needed when determining a participants MT because other stimulator intensities such as conditioning pulses and test stimuli are determined from this.

2.3.4 Recruitment Curve

As TMS intensity increases a stronger induced current is created within the brain. This stronger current is concurrent with a larger muscle response. However, once a certain intensity level is reached the muscle response no longer grows. A measurement that exhibits the growth of a muscle response as a function of TMS intensity is called a recruitment curve. Recruitment curves give investigators an indication of where the motor threshold lies, at which intensities MEPs are sensitive to change, and at which intensity MEPs no longer change. The mechanism in which increased excitability occurs is not fully understood but may be due to recruitment of neurons outside of the core neurons recruited at threshold. These additional neurons either have a higher threshold or are physically farther away from the stimulus.[56]

2.3.5 Short-latency afferent inhibition

A peripheral nerve stimulus followed by a suprathreshold TMS pulse to the motor cortex at roughly 18-21ms results in a suppression of the MEP in the first dorsal interosseous muscle (FDI).[1,66] Similarly, if the interstimulus interval between the nerve stimulation and TMS pulse is between 100-200ms, MEPs are suppressed.[66,67]

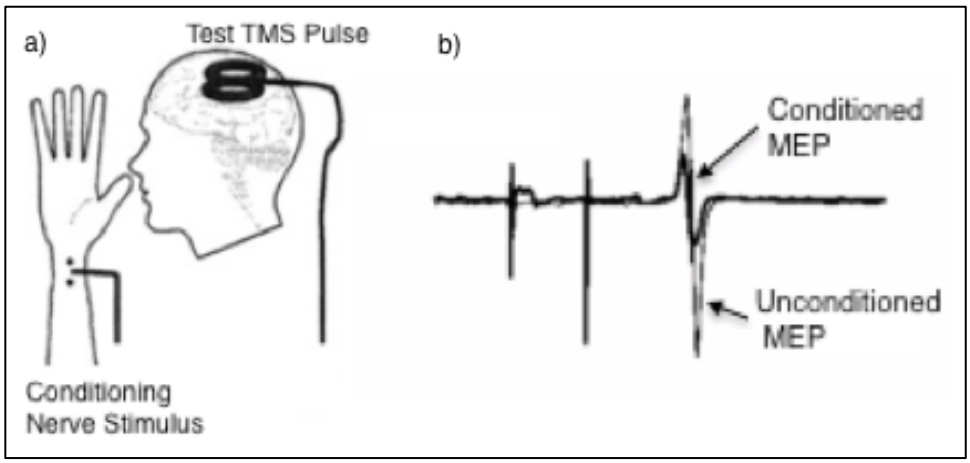

Fig 2 Illustration of the a) conditioning-test stimulus protocol and the b) resulting motor evoked potentials.
Modified from; Hallett et al., 2007&Tokimura et al., 2000

This phenomenon is known as short-latency afferent inhibition (SAI) and the interval between the stimuli are dependent on the latency of the afferent volley from the nerve stimulation to the somatosensory cortex (N20). The afferent volley can be elicited from stimulation of a cutaneous nerve or a mixed nerve.[1,68,69] SAI is modulated by cortical mechanisms since descending I-waves are decreased in amplitude after SAI and TES, which stimulates the corticospinal output neurons directly does not evoke SAI.[1,67] The exact mechanism to which SAI functions is debated, and is not known if afferent volleys travel through SI to M1 or if a direct synapse with M1 exists.[70] SAI is known to proceed through both muscarinic and GABAergic systems. Pharmacological studies show scopolamine, an anticholinergic drug, reduces SAI and increasing acetylcholine in Alzheimer's patients using rivastigmine increases SAI.[71,72] Diazepam, a $GABA_A$ modulator, increases SAI.[73] SAI is affected by nerve intensity, and the depth of SAI increases as nerve intensity increases. This is due to a greater afferent volley to the cortex, resulting in a greater inhibitory effect.[26] Nerve selection can have an effect on the SAI seen in a given muscle. In forearm muscles median nerve and ulnar nerve

stimulation show SAI on the reciprocal muscles, extensor carpi radialis and FCR respectively.[74] Hand dominance also has an effect on SAI, as in the dominant hand SAI is more pronounced.[75] SAI is thought to play an important role in cutaneomuscular reflexes in a contracting muscle by providing the early and late inhibitory effect, thus an important neural circuit in sensorimotor integration.[1]

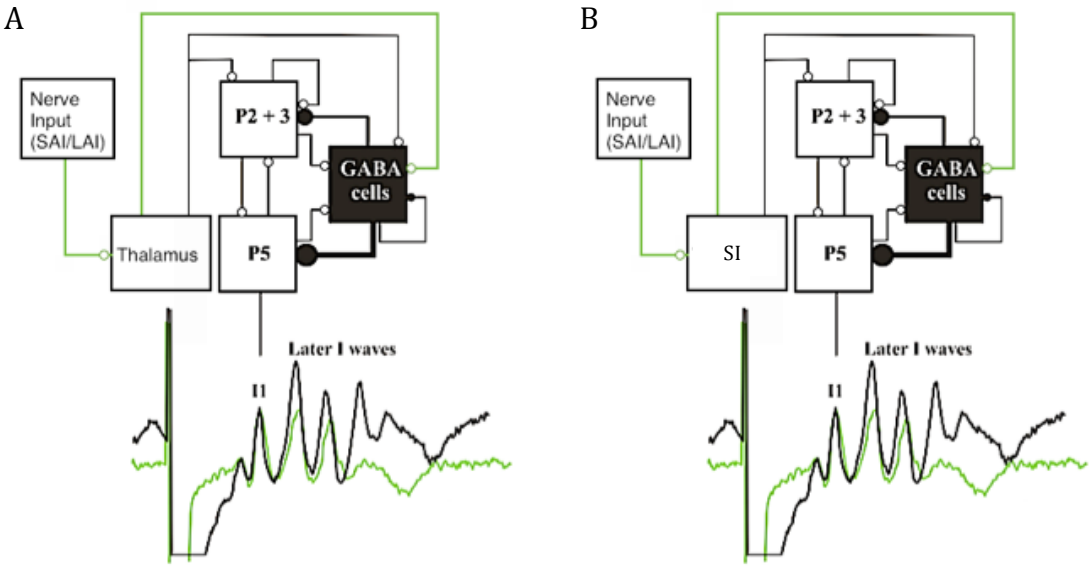

Fig 3. Illustration as to how afferent input facilitates the either A) thalamus or B) somatosensory cortex, which would both increase excite GABA cells. These GABA cells then have a greater inhibitory effect on the P2,3 and 5 interneurons, decreasing late I-waves and muscle response.
Modified from; Di Lazzaro et al., 2012.

2.4 Changes after Spinal Cord Injury

2.4.1 Spinal Cord Injury

Many different mechanisms of traumatic injury exist in which the spinal cord can be damaged resulting in variable amounts of functional loss. Three main types of incomplete

injury exist and each one effect different regions of the spinal cord causing distinct functional loss.[76] Anterior spinal cord syndrome is a common occurrence as a result of a hyperflexion injury and is associated with weakness and a loss of perception towards pain and temperature.[76] Central spinal cord syndrome is often a result of a hyperextension mechanism and is associated with weakness, loss of pain and temperature perception as well as a loss of touch discrimination and proprioception.[76] Brown-Sequard syndrome usually is caused by a stab wound is can be characterized by ipsilateral weakness, contralateral loss of pain and temperature sensation as well as ipsilateral loss of touch discrimination and proprioception.[76] Finally a complete spinal cord injury can be a result from a crush injury or a transection where the spinal cord is completely severed. A complete spinal cord injury results in a complete loss in both sensory and motor function below the level of injury. Following a spinal cord injury diagnostic imaging via magnetic resonance imaging (MRI) is performed to label the level of injury and the amount of physical damage can be quantified.[77] Functional decrements following spinal cord injury are most often assessed using the American Spinal Injury Association (ASIA) Impairment Scale. This is a comprehensive exam to determine the amount of sensory and motor loss that has occurred. All twenty-eight dermatomes are evaluated to determine the sensory loss and isometric strength tests are performed on twenty muscles to determine motor loss. The third portion of the exam is reflex testing in both upper and lower extremities. The final examination is to test whether the participant has voluntary control over the anal sphincter. This is an important step in patients who have a severe injury because any voluntary control over the sphincter means the injury is incomplete. After both diagnostic imagining and ASIA assessments are performed patients injury level as well as severity of injury will be known.[78]

2.4.2 Cortical Plasticity Following Damage to Central Nervous System

An alteration to the inputs and outputs of the cortex can lead to plasticity or cortical reorganization[79]. An increase or decrease in the use of a particular limb or muscle will result in a plastic change within the cortex that translates to a selective allocation of area to represent this limb or muscle.[79,80] Following a spinal cord injury a loss of motor and sensory function below the level of injury is seen.[11,13] This decrease in function leads to an organizational change within the somatosensory cortex and the motor cortex. Specifically, within SI areas responsible for receiving input from sensory deprived areas are taken over by surrounding areas where sensory input is still intact.[11,12] Topographical reorganization is not as drastic within M1 and an increase in activation is seen when performing movements.[11,13] Since projections between SI and M1 are extensive and are topically organized, plasticity within these areas can have an effect on cortical mechanisms such as SAI and LAI.

2.4.3 How can Afferent Input Change following SCI?

Afferent information and how it is processed changes after a spinal cord injury. Compound motor action potentials (CMAP) and sensory nerve action potentials (SNAP) from nerve conduction studies are decreased in amplitude at the level of injury immediately following injury, but are not changed above and below the level of injury (Spinal Cord Medicine). The function of spinal inhibitory circuits decrease after a spinal cord injury.[81] H-Reflexes, an indirect method of measuring spinal inhibitory circuits,

decrease following SCI.[82,83] As a result afferent volley's to the cortex are decreased in amplitude and increased in latency.[9]

2.4.4 How can Motor Evoked Potentials Change following SCI?

Descending efferent pathways are damaged in those who have a spinal cord injury. In an incomplete spinal cord injury the degree of connectivity differs muscle to muscle and voluntary control may be absent in some muscles. This does not mean connectivity from the cortex is absent.[10] When determining motor evoked potentials by use of TMS we see responses are smaller and delayed when compared to uninjured controls.[10,11,84] It is possible however to illicit a motor twitch from muscles with no volitional control.[10] This uncovers the ability for TMS to determine muscles that are candidates for functional recovery.

2.4.5 How can Motor Threshold Change following SCI?

Active motor threshold after spinal cord injury can be altered. AMT is increased following an SCI. RMT is also higher in spinal cord injury when compared to uninjured controls.[11] The degree of spinal atrophy is positively correlated with motor thresholds as spinal cord atrophy increases motor thresholds increase. Concluding efferent pathway continuity might be the reason for the change in active motor threshold.[84] However, one case study was performed on a single participant and a lower RMT was found. The authors reasoned lower RMT is a result of a reduction in the inhibitory function of the motor cortex.[85]

2.4.6 How can Afferent Regulation (SAI) Change following SCI?

The depth of short latency afferent inhibition is correlated with the intensity of the afferent stimulus.[26] A decrease in afferent input would serve to reduce the amount of SAI. After spinal cord injury the amount of afferent volleys able to make it to the cortex is reduced, as shown by a decrease in latency and amplitude of SEP's.[9] SAI has been shown to decrease in those who have an SCI for a given nerve intensity.[86] This may occur due to less afferent volleys traveling to the cortex as degree of disinhibition was related to severity of injury.[9,26,86] Another explanation could be due to the reduction of spinal inhibition that occurs after spinal cord injury.[81,86]

Chapter 3: Experiment 1

Alterations to the short-latency afferent inhibition circuit in chronic spinal cord injury

3.1 Introduction

Neuroplasticity in sensorimotor cortex follows spinal cord injury (SCI) and reflects the location and extent of damage in ascending and descending pathways. In humans, the integrity of sensorimotor cortical paths may be assessed via short-latency afferent inhibition (SAI) whereby the afferent volley elicited by peripheral nerve stimulation reduces the amplitude of the motor evoked potential (MEP) elicited by Transcranial magnetic stimulation (TMS) over the primary motor cortex (M1) [29,67]. SAI is considered a cortically generated circuit evoked by the arrival of the peripheral afferent volley in the cortex and is mediated via neuronal circuitry within M1 [29].

The magnitude of SAI depends on the integrity of afferent transmission and the activity within the cortical circuitry that mediates SAI. If, in SCI, the afferent volley arriving at the cortex is reduced due to damage to the ascending pathway, a reduction in SAI is expected as the depth of SAI decreases with lower nerve stimulation intensities [26]. Additionally, substantial plastic changes may occur after an SCI in either M1 or SI. Within M1 the cortical areas responsible for controlling the muscles below the level of injury decrease in size and the muscles above the level of injury increase in size [87]. Decreasing the neurons responsible for controlling muscles below the level of injury may decrease the ability for an afferent stimulus to condition those neurons and elicit SAI. Following upper limb deafferentation somatosensory and thalamic areas atrophy in

primates [88] and may decrease extensive projections from SI to M1[52,53] , thus decreasing SAI. One study in chronic SCI demonstrated a reduction in SAI in the contracted tibialis anterior muscle [86], although the mechanism(s) for this effect remain unclear. At present, there are several unstudied questions regarding SAI in SCI that include whether abnormalities exist in upper limb muscles, whether they occur when the muscle is in the relaxed, non-contracted state, and whether the magnitude of SAI is different in SCI versus uninjured controls.

Determining whether SAI is reduced in SCI compared to controls is important since SAI is a sensorimotor circuit that is implicated in movement and plays an important role in the concept of surround inhibition [3,27,28]. Further, reductions in SAI in other clinical populations have been implicated in sensory driven long-term potentiation to motor cortex, which may promote motor learning and recovery [7]. In the present study, SAI was examined in the flexor carpi radialis (FCR) muscle in chronic cervical SCI and uninjured controls in both the non-contracted and contracted muscle states. In uninjured controls, SAI is observed in the FCR muscle when the interval between the nerve and cortical stimulation is between 13-20 ms [74]. Relative to other muscles of the upper limb, FCR function is often partially retained [10] after SCI which offers the opportunity to study its afferent regulation in both the contracted and non-contracted states. Further, we explored whether alterations in the SAI circuit would be due to changes in the transmission through afferent pathways by measuring the amplitude of sensory nerve action potentials (SNAPs) and somatosensory evoked potentials (SEPs) and transmission of efferent pathways through MEPs. We hypothesized that, MEPs will be reduced due to damage in the efferent fibers, SAI will be reduced due to reduced afferents arriving in the

cortex and SEPs will be altered due to reduced afferents arriving in the cortex. Our data indicate that SAI is indeed reduced in SCI compared to uninjured controls in the contracted and non-contracted muscle. However, our data suggest reduced afferents may contribute to reduced SAI but we cannot discern any further contributions from neuroplasticity within SI and/or M1.

3.2 Methods

Participants

Thirteen limbs from eight adults with cervical spinal cord injury were studied (7 males; mean age = 30.8 +/- 2.4, Asia B-D). Table 1 provides demographic, lesion and medicinal information for all SCI participants. All SCI participants were capable of performing volitional wrist flexion in the limbs tested. One participant, P003, dropped out due to medical reasons and was not able to finish the study. Therefore, twelve limbs from seven adults with SCI (6 males; mean age = 30.7 +/- 2.6, Asia B-D) were included in our results. Twelve dominant limbs from aged-matched uninjured participants were studied for comparison (8 males; mean age = 29.15 +/- 5.33). The Hamilton Integrated Research Ethics Board approved the study. All participants provided written consent prior to participation. Where applicable SCI subjects were tested bilaterally, and limbs were treated as separate individuals as performed elsewhere [86,89].

Electromyography (EMG) Recordings

EMG was collected from the FCR using 9 mm diameter Ag-AgCl surface electrodes in a belly-tendon fashion. Manual palpation was performed during contraction and rest in all participants to locate the muscle belly. The active electrode was placed on average 3 cm

distal and 2 cm lateral to the medial epicondyle. The reference electrode was placed over the tendons of the wrist and the ground electrode was placed over the medial styloid process of the wrist. EMG signals were amplified at a gain of 1000, band pass filtered with a high pass of 20Hz and low pass of 25000Hz and collected (CED 1401) for offline analysis (Signal v5).

Transcranial magnetic stimulation and NeuroNavigation

TMS was performed using a 50 mm inner diameter figure-of-eight branding coil connected to a Magstim 200^2 stimulator. Motor hotspot for FCR was determined as the location providing the most reproducible and largest MEP in the FCR muscle. The coil was positioned 45 degrees to the mid-sagittal line to induce current in a posterior to anterior direction. Resting motor threshold (RMT) was determined at this location and was defined as the lowest stimulator intensity required to elicit MEPs $\geq 50\mu V$ in 5 out of 10 consecutive trials. Active motor threshold (AMT) was defined as the lowest stimulator intensity required to elicit MEPs of distinguishable from background contraction levels as determined by visual inspection in 5 out of 10 trials. Brainsight Neuronavigation was used to target and track the location of these motor hotspots.

Corticospinal output

MEP recruitment curves were obtained in the active and resting FCR by stimulating the FCR hotspot at TMS intensities as a percentage of maximum stimulator output (MSO). The initial TMS intensity was set to 10% MSO and increased in increments of 10% every three stimulations. The MEP at each MSO was determined as the average of the three stimulations. $MEP_{halfmax}$ was identified from the recruitment curve as the stimulation

intensity where half of the maximal response was recorded. This intensity was further refined and confirmed through ten subsequent trials.

Short-latency afferent inhibition (SAI)

The median nerve at the elbow was stimulated just lateral and proximal to the medial epicondyle, slightly medial to the medial edge of bicep. The median nerve was stimulated at 1.2 x motor threshold (for twitch in FCR) using a bar electrode with the cathode proximal (0.2 ms square wave pulse, SD9 stimulator, Grass Technologies). TMS was delivered over the FCR hotspot at an intensity to evoke $MEP_{halfmax}$ in the active or resting FCR. This intensity was adjusted online to maintain a half-max response in the active or resting FCR. To test SAI of FCR, the median nerve was stimulated at three interstimulus intervals in advance of the TMS pulse: 15, 20, 25 ms. These ISIs approximate the arrival of the afferent volley in somatosensory cortex at ~ 15 – 18 ms following median nerve stimulation at the elbow [74] and account for additional delays due to traumatic injury to the ascending pathways. SAI was tested in each limb while the FCR was relaxed (i.e. rest) or actively contracted to ~ 20% MVC (active). Each ISI was repeated 10 times and 'TMS only' was repeated 20 times.

To assess the background EMG during afferent regulation measured at rest, the pre-stimulus (38 ms) area of the rectified EMG was measured for each epoch. This value was averaged for each ISI and TMS only trials. To assess the background EMG during afferent regulation measured in active FCR, the pre-stimulus (38 ms) area of the rectified EMG was measured for each epoch and normalized to a 38 ms window of the individual's maximum voluntary contraction. To determine the maximum voluntary

contraction for FCR participants were asked to maximally contract the forearm during wrist flexion. Three trials (each 3 s) were performed and separated ~20 s, to allow EMG to fall back to baseline while allowing participants to reach maximum EMG responses in each subsequent trial as confirmed statistically (two-way ANOVA with factor trial (first, second, third) and group (SCI, group) indicate all p-values > 0.05). MVC was marked on an oscilloscope and was used to calculate 20% MVC to which a bright line was displayed. During afferent regulation in active FCR (which required 20% MVC), the EMG from FCR was displayed as bright line on the oscilloscope and participants would match the position of the FCR EMG line to the experimenter-defined 20% MVC target line.

Somatosensory evoked potentials and sensory nerve action potentials

SEPs were acquired at C3' and referenced to Fz. The ground electrode was placed over the clavicle. SEPs were evoked through MN stimulation at the elbow just lateral and proximal to the medial epicondyle, slightly medial to the medial edge of bicep. The median nerve was stimulated at 1.2 x motor threshold (for twitch in FCR) using a bar electrode with the cathode proximal (0.2 ms square wave pulse, DS7AH, Digitimer). and were averaged over 500 sweeps. Sensory nerve action potentials (SNAPs) were evoked by stimulation of the median nerve at the wrist and recorded using surface electrodes placed at the elbow with one located above the medial epicondyle and the other just below the bicipital groove. Both EEG and SNAP signals were amplified at a gain of 10000, band pass filtered with a high pass of 2Hz and a low pass of 25000Hz and collected (CED 1401) for offline analysis of the amplitude (N20-P25, SNAP) and latency (Signal v5). Since median nerve is stimulated at the elbow the latency of the N20 is

expected to fall around 15 ms as observed elsewhere [74]. Where applicable SEPs were collected bilaterally.

Data Analysis

All data was collected and stored for offline analysis using Signal v5 (Cambridge Electronic Design, UK). The area of the rectified MEP was measured. Afferent regulation was expressed as the ratio of the conditioned to unconditioned MEP (i.e. $MEP_{nerve\text{-}TMS}/MEP_{TMS}$). AMT and RMT were subject to unpaired one-tailed t-tests to test the hypotheses that each threshold measure would be greater in SCI compared to controls as observed elsewhere [90]. For MEP recruitment curves, a two-way ANOVA was performed with INTENSITY as the within-subject factor (10 levels; 10%-100%) and between-subject factor GROUP (2 levels; SCI, uninjured). For SAI, normalized MEP area ($MEP_{nerve\text{-}TMS}/MEP_{TMS}$) was subjected to a two-way ANOVA performed using within-subject factor ISI (3 levels; Test, 15, 20, 25) and between-subject factor GROUP (2 levels; SCI, uninjured). Background EMG was subject to two-way ANOVAs with either ISI (4 levels; Test, 15, 20, 25) or INTENSITY (10 levels; 10, 20, 30, 40, 50, 60, 70, 80, 90, 100) as the within-subject factor and between-subject factor GROUP (2 levels; SCI, uninjured). SEP latency and amplitudes were subject to two-way ANOVAs with STATE (2 levels; active, rest) as the within-subject factor and GROUP (2 levels; SCI, uninjured) as the between-subject factor. Group averaged SNAP amplitude was subject to unpaired two-tailed t-test. Post-hoc Tukey's tests were conducted following significant ANOVA effects. Significance was set at $p < 0.05$ and if the assumptions of sphericity were not met, Greenhouse-Geisser corrections were used.

3.3 Results

Twelve limbs from seven adults with cervical SCI were studied and reliable, robust MEPs were obtainable in FCR during active contraction. However, only 9 limbs provided reliable, robust MEPs in FCR during rest and subsequent analyses were performed only on these limbs for measures of RMT, MEP recruitment curve at rest, and afferent regulation at rest. Data from all twelve limbs were included in AMT, MEP recruitment curve during active contraction and afferent regulation during active contraction.

Threshold & corticospinal output

Group-averaged RMT and AMT are shown in Figure 4A and B. RMT was not different between groups ($p=0.87$) and AMT was significantly higher in SCI ($p=0.002$).

MEP recruitment curves with FCR at rest are shown in Figure 4C. Two-way ANOVA revealed a significant effect of INTENSITY ($F_{(1.29,25.51)}=17.70$; $p<0.001$) and no GROUP ($F_{(1,19)}=1.85$; $p=0.189$) or GROUP*INTENSITY interaction ($F_{(1.29,25.51)}=2.085$; $p=0.16$). Background EMG was not different between groups ($F_{(1.085,18.44)}=1.849$; $p=0.19$).

MEP recruitment curves with FCR contracted to ~20% MVC are shown in Figure 4D. Two-way ANOVA revealed significant effects of INTENSITY ($F_{(1.93,42.38)}=67.42$; $p<0.001$), GROUP ($F_{(1,22)}=32.82$; $p<0.001$) and GROUP*INTENSITY ($F_{(1.93,42.38)}=23.91$; $p<0.001$). MEPs were greater from 40 to 100% MSO in controls compared to SCI (Tukey's, $p<0.05$) while background EMG was not different between groups ($F_{(3.056,58.07)}=0.98$; $p=0.41$).

SAI in FCR

a) Non-contracted, relaxed FCR

Figure 5A displays the group-averaged SAI data in resting FCR for SCI and controls. Values below the horizontal line indicate afferent inhibition of the MEP. Two-way ANOVA revealed a significant ISI*GROUP interaction ($F_{(2,32)}$=4.31; p=0.022) with no ISI ($F_{(2,32)}$=2.96; p=0.066) or GROUP ($F_{(1,16)}$=0.607; p=0.447) effects. SAI was significantly reduced for SCI versus controls (Tukey's, $p<0.05$) at the 15 ms ISI that corresponds to SAI for stimulation of the median nerve at the elbow [74]. Individual traces of 15 ms SAI (conditioned and unconditioned MEPs) from individual participants are shown in Figure 5B. Background EMG was not significantly different during SAI testing (GROUP ($F_{(1,19)}$=0.315; p=0.581, ISI*GROUP ($F_{(1.44,27.34)}$=1.11; p=0.326)).

b) Contracted, Active FCR

Figure 5C displays the group-averaged SAI data in active FCR for SCI and controls. Two-way ANOVA revealed a significant ISI*GROUP interaction ($F_{(1.54,35.43)}$=6.35; p=0.008) and no ISI ($F_{(1.54,35,43)}$=0.48; p=0.573) or GROUP ($F_{(1,23)}$=3.27; p=0.083) effects. SAI was significantly reduced in SCI versus controls at 15, 20 and 25 ms ISI (Tukey's, $p<0.05$). Traces of 15 ms SAI from individual participants are plotted in Figure 5D. Background EMG was not significantly different during SAI testing (GROUP ($F_{(1,17)}$=2.42; p=0.138), ISI*GROUP ($F_{(1.08,18.45)}$=3.9; p=0.061).

Somatosensory evoked potentials and Sensory nerve action potentials

Figure 6A displays the group-averaged latency in both the active and resting FCR for SCI and controls. Two-way ANOVA revealed no interaction between STATE*GROUP ($F_{(1, 12)}$=0.153; p=0.702), no effect of STATE ($F_{(1, 12)}$=0.646; p=0.437) and a near significant

GROUP effect ($F_{(1,12)}$=4.009; p=0.068). The latency observed in both the SCI and control groups is similar to the latency of other studies performing median nerve stimulation at the elbow, ~15 ms [74]. Figure 6B displays the group-averaged N20-P25 amplitude in both the active and resting FCR for SCI and controls. Two-way ANOVA revealed no interaction ($F_{(1, 12)}$=0.2; p=0.662) and no main effects (STATE; $F_{(1, 12)}$=1.82; p=0.202, GROUP; $F_{(1,12)}$=0.038; p=0.849). Figure 6C displays the group-averaged SNAP amplitude in both groups. SNAP amplitude was significantly reduced in the SCI group compared to controls (unpaired two-tailed t-test, p=0.045).

3.4 Discussion

The present study revealed abnormalities in the magnitude of SAI in SCI. Compared to uninjured controls, SAI is reduced in SCI in both the contracted and relaxed FCR muscle. In SCI, corticospinal output to FCR is different from that of controls only during active contraction of the muscle. Further, in our sample of participants, SEP amplitude, which reflects the magnitude of the cortical afferent volley arriving at the primary somatosensory cortex, is not different between groups and therefore activation of SI may not explain reduced SAI in SCI. However, measurements of the peripheral afferent volley (SNAPs) show reductions in our SCI group and may imply reduced afferents leading to alterations in SAI.

Mechanisms that mediate SAI and its reduction

The SAI circuit is very complex and the exact mechanisms that underpin its origin are relatively unknown. SAI is a cortically mediated circuitry modulated by the late I-wave generating neurons within M1 as peripheral nerve stimulation reduces the amplitude of

the descending I3 wave [1]. SAI can be altered through many different mechanisms. SAI is increased with an increase in the peripheral afferent volley [26] and decreased with an increase in the amplitude of the descending efferent volley [91]. Further, any modifications to the cortico-cortical projection from SI to M1 may potentially modify SAI, and changes to the late I-wave circuitry within M1 may alter SAI strength. Alterations to any one of these or their combination may result in changes to the strength of the SAI circuitry. In our study we observed a decrease in the peripheral afferent volley in our SCI group without changes in SEP amplitude. It is possible that our cohort had ~ 50% of their afferent tracts spared since SEP amplitudes saturate at approximately 50% of the afferent volley maximum [46]. Further, spinal cord injury may result in neuroplasticity within SI [88,92] that may lead to alterations in the integrity of the cortico-cortical projection from SI to M1, and possible neuroplasticity to the I-wave circuitry within M1. Therefore, in our study we characterized the afferent volley and corticospinal projections, and our findings suggest that each of these may contribute to alterations in SAI depending on the state of the muscle. Importantly, we should not exclude potential contributions from neuroplasticity that may be detected using alternate imaging methods.

Non-contracted FCR

With the FCR muscle relaxed, we observed similarities between SCI and controls in RMT, MEP recruitment curve and SEPs. In contrast, our SCI group showed ~ 26% reduction in SAI compared to controls; in fact SAI was abolished in the SCI group and ~ 43% reduction in SNAP in SCI compared to controls. This effect occurred specifically at the 15 ms interstimulus interval that corresponds to the latency of the cortical arrival of

the afferent volley (Figure 3A). Reduced SAI does not result from abnormalities in the magnitude of the afferent volley terminating in SI since the amplitude of the N20-P25 is within the normative range [93] and not different from our control group but may be explained by the reduced afferent volley in the periphery. Further, abolished SAI does not result from reduced corticospinal/spinal output since the MEP recruitment curves are not substantially different between groups. Therefore, the absence of SAI is likely to result from changes in the peripheral afferent volley, neuroplasticity altering the somatosensory to M1 projection (i.e. cortico-cortical) and/or the intrinsic M1 neuronal circuitry that mediates SAI.

Contracted FCR

With the FCR muscle voluntarily contracted, we observed several differences between SCI and controls. First, AMT was higher in SCI compared to controls. This effect may result if active contraction excites fewer neurons and/or the capacity to reduce the membrane potential is compromised in the SCI group. Increased AMT may relate to abnormalities in the function of voltage-gated Na^+ channels [62] that regulate axon excitability [94]. Drugs that block voltage-gated Na^+ channels increase motor threshold [95-98] and this may be a mechanism to explain elevated AMT in SCI. Second, compared to controls, MEP amplitude in SCI during active contraction was reduced from 40 – 100% MSO, and within this range MEPs were not increased as a function of TMS intensity. One potential explanation for the reduction in MEP amplitude during active contraction may relate to alterations in the activity of the $GABA_A$ receptor. In support of this suggestion the $GABA_A$ mediated SICI circuit is reduced in SCI participants during active contraction of the tibialis muscle [89]. Further, $GABA_A$ agonists reduce the slope

and amplitude of MEPs [99-104]. Therefore, it remains unclear whether $GABA_A$ receptor function is increased or decreased in our SCI population. Our MEP recruitment curve data, however, indicate that alterations likely exist in $GABA_A$ function in individuals with SCI. Further, considering that both AMT and active corticospinal output are reduced, individual with SCI may have abnormalities in the neural mechanisms required to bring upper and/or lower motor neurons closer to firing threshold through active contraction.

During active contraction, SAI in SCI was reduced compared to controls; in fact the SCI group appears to show short latency afferent facilitation. However, paired t-tests on these data do not show significant facilitation (15 ms: $p=0.487$; 20 ms: $p=0.468$; 25 ms: $p=0.344$). These data are consistent with SAI reductions in the tibialis anterior muscle in SCI seen elsewhere [86]. SAI was abolished in SCI at latencies corresponding to the cortical termination of the afferent volley (i.e. 15 ms) and beyond but the amplitude of N20-P25 was not different between groups. SNAPs were unattainable during active contraction because muscle activity contaminated the SNAP traces. Therefore we cannot comment to the integrity of the afferent volley during active contraction but can estimate based on data in the resting limb. Therefore, reduced SAI during active contraction may be explained by reduced integrity of the ascending and/or descending pathway, neuroplasticity within SI [88], in the somatosensory to M1 projections and/or to the intrinsic motor circuitry that mediates SAI.

Limitations

We did not attempt to test individuals with SCI in their non-medicated state to avoid spasticity and other complications. We consider the contribution of baclofen, a $GABA_B$ agonist, minimal since the SAI circuitry is modulated via acetylcholine and/or $GABA_A$ [62,73,105,106]. Our study primarily focused on the SAI circuit and did not test short-interval intracortical inhibition a measure of $GABA_A$ function or measures of $GABA_B$ function including the contralateral silent period and long-interval intracortical inhibition and as such cannot make conclusions based on $GABA_A$ or $GABA_B$ function. Further, neuroimaging techniques such as high-field functional magnetic resonance imaging may reveal the neuroplastic effects within either SI or M1 that may reduce SAI.

3.5 Conclusions

The data presented support the existence of neuroplasticity changes that have altered the cortical circuit that mediates SAI. Further, our data suggest that, in chronic tetraplegia, activating the upper and/or lower motorneurons via voluntary muscle contraction underestimates the magnitude of the residual corticospinal output to the FCR muscle. Artificial stimulation of the corticospinal tract via TMS in the relaxed muscle exposes the greater, residual capacity of the corticospinal tract. This suggestion is supported by the finding that MEPs in SCI are obtainable via TMS in muscles that are incapable of voluntary contraction [10].

In conclusion, our study reveals novel findings of aberrant SAI cortical circuitry that outputs to the FCR muscle in chronic SCI. This circuit is abolished in both a relaxed and contracted muscle, an effect that exists despite investigating a well-recovered muscle and

nerve combination. MVC, RMT, and SEPs are all similar between the two groups and collectively argue for functional SAI. However, reduced SAI is supported by reduced peripheral afferents as shown and may be additionally explained by neuroplastic changes in cortical circuitry that mediates SAI. This work leads to a new avenue of research in chronic SCI populations aimed at increasing corticospinal output to active FCR and by increasing SAI, a sensorimotor circuit implicated in the control of movement [2,3,28], through altering either peripheral volley, projections from SI-M1 and/or the intrinsic neurons in M1 responsible for controlling SAI.

3.6 Table 1: Demographics

Subject ID	Injury Level	Years Post Injury	Cause of Injury	ASIA Score	Medications	Limb Tested
P001	C4-C5	11	Traumatic	C	Baclofen	Right & Left
P002	C3	2	Surgical	C	Baclofen	Right & Left
P004	C5-C6	3	Traumatic	C	Baclofen, Soflax, Gabapentin, Pantopraxole, Senkot, Detrol	Right & Left
P005	C4	16	Traumatic	C	Oxycotin, Hydromorphine, Glucosamine	Right
P006	C5	14	Traumatic	B	Axid, Collase, Ditropan, Baclofen	Right & Left
P007	C3-C4	7	Traumatic	B	Fentinal Patch, Pregabilin, Baclofen, T.Zanodine, Oxybutin, Hyrdromorphine	Right
P008	C5	9	Traumatic	D	Benadryl, Percocet	Right & Left

Figure 4

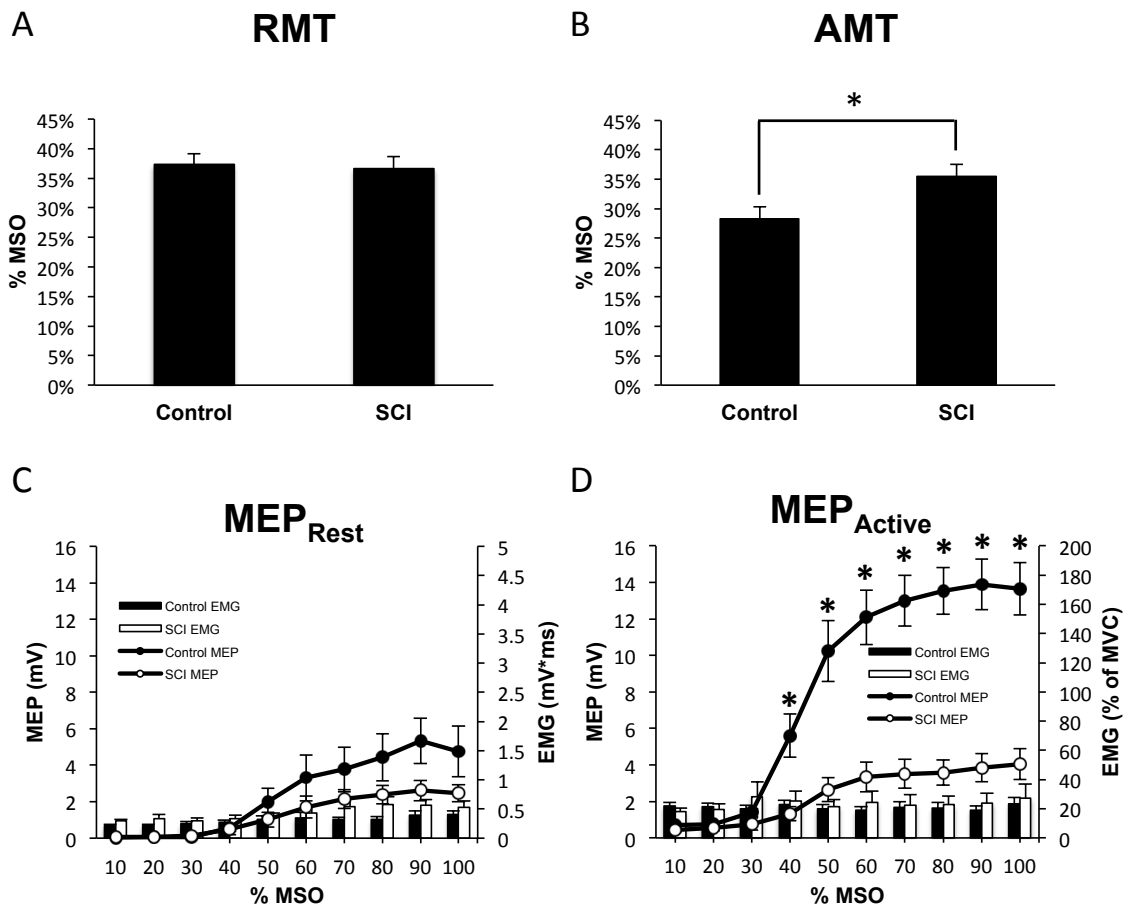
A
RMT
% MSO
45%
40%
35%
30%
25%
20%
15%
10%
5%
0%
Control
SCI
B
AMT
*
% MSO
Control
SCI
C
MEP Rest
MEP (mV)
EMG (mV*ms)
Control EMG
SCI EMG
Control MEP
SCI MEP
% MSO
D
MEP Active
MEP (mV)
EMG (% of MVC)
Control EMG
SCI EMG
Control MEP
SCI MEP
% MSO

Figure 5

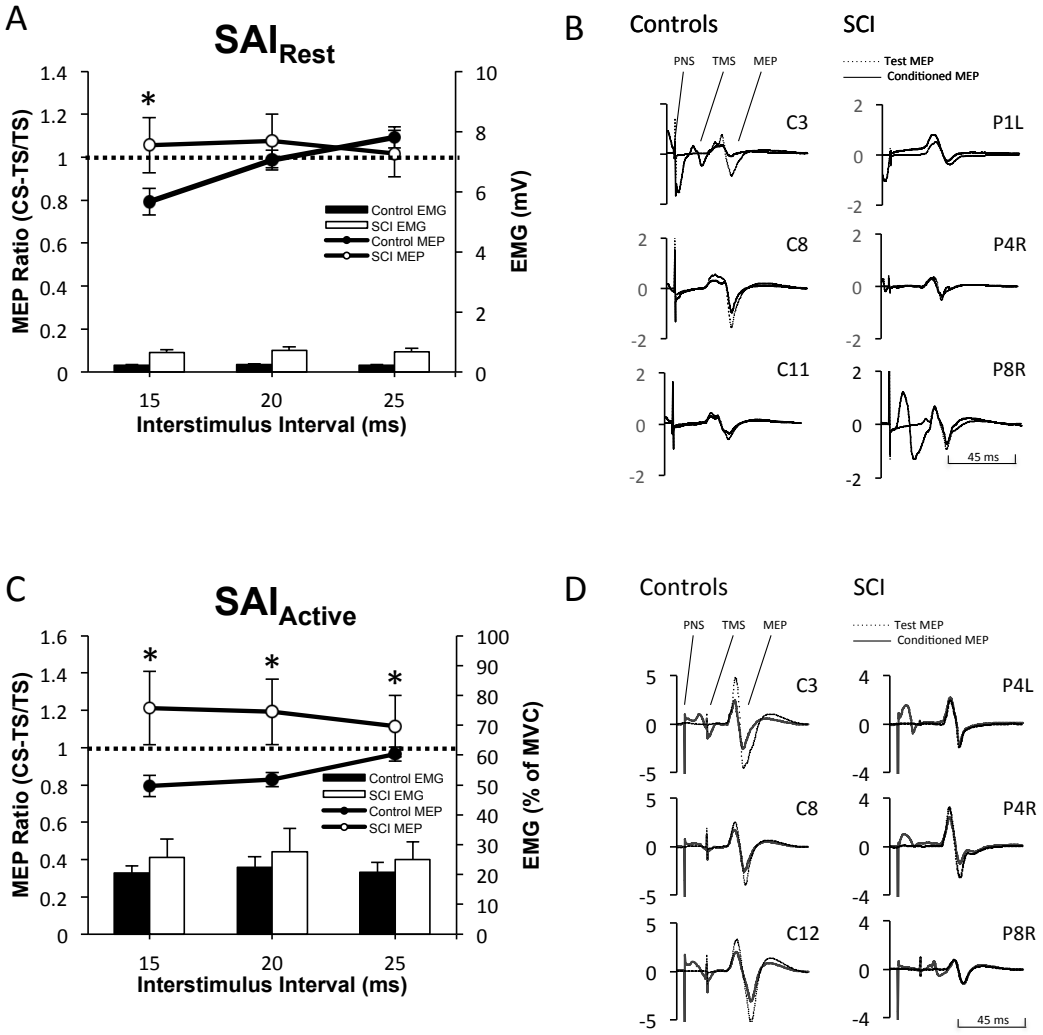
A
SAI Rest
MEP Ratio (CS-TS/TS)
EMG (mV)
Control EMG
SCI EMG
Control MEP
SCI MEP
Interstimulus Interval (ms)
B
Controls
SCI
PNS
TMS
MEP
Test MEP
Conditioned MEP
C3
C8
C11
P1L
P4R
P8R
45 ms
C
SAI Active
MEP Ratio (CS-TS/TS)
EMG (% of MVC)
Interstimulus Interval (ms)
D
Controls
SCI
C3
C8
C12
P4L
P4R
P8R
45 ms

Figure 6

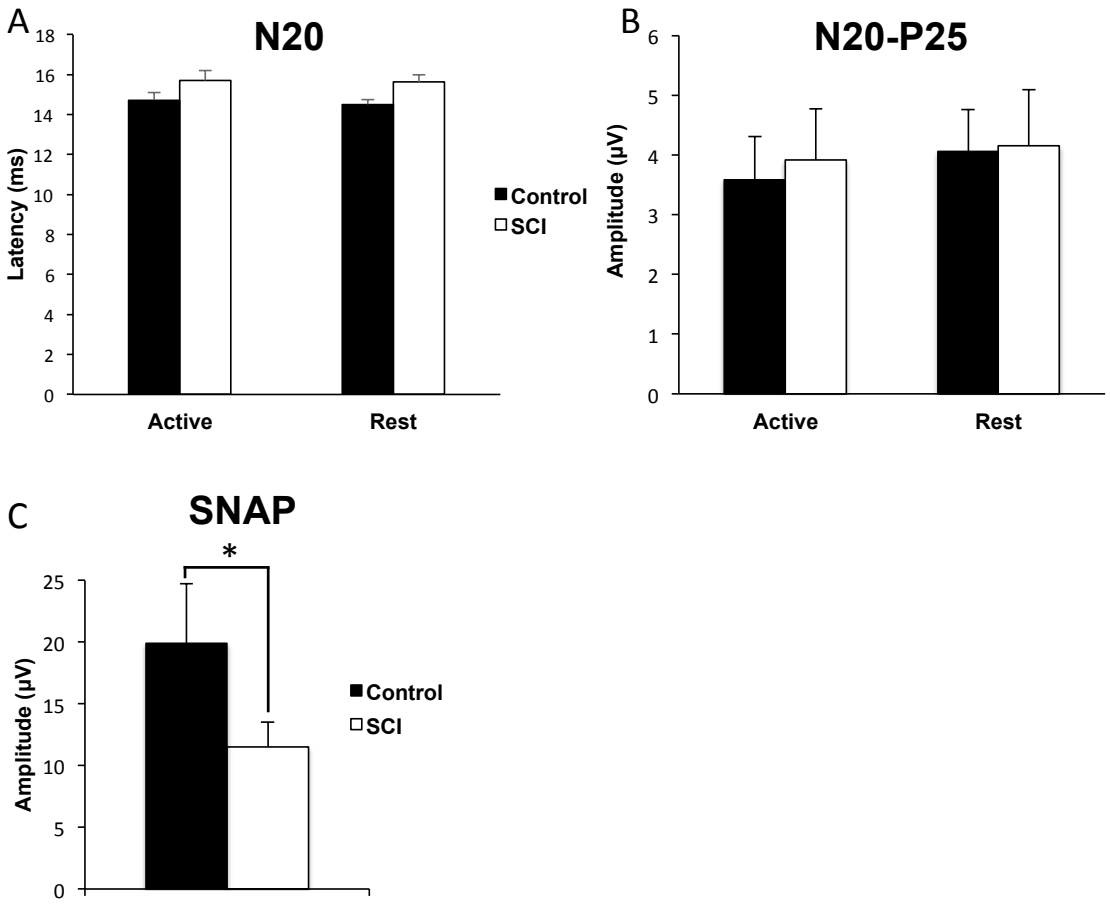
A
N20
Latency (ms)
18
16
14
12
10
8
6
4
2
0
Active
Rest
Control
SCI
B
N20-P25
Amplitude (µV)
6
5
4
3
2
1
0
Active
Rest
C
SNAP
*
Amplitude (µV)
25
20
15
10
5
0
Control
SCI

Figure Legends

Figure 4. Corticospinal output to FCR A) Group-averaged resting motor threshold (with standard errors) as a function of absolute TMS stimulator intensity in %MSO tested in both groups (n=9 SCI, n=9 controls). **B)** Group-averaged resting motor threshold (with standard errors) as a function of absolute TMS stimulator intensity in %MSO tested in both groups (n=12 SCI, n=12 controls). **C)** MEP recruitment curve in non-contracted FCR (n=9 SCI, n=9 controls). Group-averaged MEP amplitudes are represented in the line graphs (with standard errors). Histograms represent background activity in absolute terms (with standard error). **D)** MEP recruitment curve in contracted FCR (n=12 SCI, n=12 controls). Group-averaged MEP amplitudes are represented in the line graph with standard errors. Asterisks represent group differences in MEP amplitude. Histograms represent background contraction expressed as a percent of their MVC (with standard error).

Figure 5. SAI in FCR A) Group-averaged SAI in non-contracted, resting FCR (n=9 SCI, n=9 controls) shown as the ratio of the conditioned to unconditioned (i.e. TS alone) is represented in the line graphs (with standard error). Asterisks indicate where SAI is reduced in SCI compared to controls, 15 ms. Histograms represent background activity in absolute terms (with standard error). **B)** Individual examples of SAI at 15 ms ISI. Averaged MEP amplitude at 15 ms ISI and TS alone for three control and three SCI limbs. Conditioned MEP is shown as solid black and test MEP (i.e. TS alone) as dashed line. Participant codes shown. Peripheral nerve stimulation (PNS), transcranial magnetic stimulation (TMS) and motor evoked potential (MEP). **C)** Group-averaged SAI in contracted, active FCR (n=12 SCI, n=12 controls) shown as the ratio of the conditioned

to unconditioned (i.e. TS alone) is represented in the line graphs (with standard error). Asterisks indicate where SAI is reduced in SCI compared to controls, 15, 20 and 25 ms. Histograms represent background contraction expressed as a percent of their MVC with standard error. **D)** Individual examples of SAI at 15 ms ISI. Averaged MEP amplitude at 15 ms ISI and TS alone for three control and three SCI limbs. Conditioned MEP is shown as solid black and test MEP (i.e. TS alone) as dashed line. Participant codes shown. Peripheral nerve stimulation (PNS), transcranial magnetic stimulation (TMS) and motor evoked potential (MEP).

Figure 6. Somatosensory evoked potentials and sensory nerve action potentials SEPs were evoked via median nerve stimulation at the elbow, lateral and proximal to the medial epicondyle, slightly medial to the medial edge of bicep. SEPs were collected from 7 limbs from 4 SCI participants and from 7 uninjured controls. SEPs were collected and analyzed in both the active, where participants were asked to hold an isometric contraction equal to ~ 20% MVC and in the resting, where participants relaxed their forearm, states. Sensory nerve action potentials were evoked via median nerve stimulation at the wrist just lateral to the palmar tendons of the wrist and were recorded over the median nerve at the elbow. **A)** Group-averaged SEP latency in both the contracted, active, and non-contracted, resting, FCR for both SCI and controls. ANOVA revealed no significant differences between the groups ($p=0.068$) although a trend is emerging for longer SEP latency in the SCI group. The latency in both the SCI (~ 15.6 ms) and control (~ 14.7 ms) group are consistent with previous literature showing latency from this location being 15.4 ms[74]. **B)** Group-averaged N20-P25 amplitude in both the contracted, active, and non-contracted, resting, FCR for both SCI and controls. ANOVA

revealed no significant differences between the groups (p=0.849). **C)** Group-averaged SNAP amplitude in the non-contracted, resting, FCR for SCI and controls. Unpaired two-tailed t-tests revealed significant differences between the two groups (p=0.045).

Chapter 4: Experiment 2

Relationship between median nerve stimulation and indices of somatosensory function

4.1 Introduction

Neural activity within the primary somatosensory cortex (SI) is commonly assessed via electrical stimulation of the median nerve. Increasing electrical nerve stimulation intensity recruits larger afferent volleys as measured by the gain in sensory nerve action potentials (SNAPs), and is maximal when all afferent fibers within the nerve are recruited [107,108]. Using median nerve stimulation, somatosensory evoked potentials (SEPs) allow excitation and inhibition to be quantified within SI while short-latency afferent inhibition (SAI) measures the influence of the somatosensory afferent volley on neural circuits within primary motor cortex (M1). Such measures are valuable indices of sensorimotor function for intervention-based studies that aim to alter neural activity in healthy and/or clinical populations. Understanding the relationship between the afferent volley and measures of sensorimotor function is essential for designing effective research studies, and, understanding their interrelatedness will provide insight into the neural mechanisms that mediate each circuit.

There is an increasing stimulus-response relationship between median nerve evoked SNAPs and the somatosensory evoked potential (SEP) recorded over SI such that the N20-P25 increases to ~ 50% of the maximum SNAP (i.e., $SNAP_{max}$) [38,46]. Increases in SNAP amplitude beyond ~ 50% are hypothesized to be the result of antidromic activity in

motor fibers [38,46] that do not yield any further changes to SEPs [38,46]. Therefore, these data suggest that, for median nerve stimulation at ~ 50% of $SNAP_{max}$, all sensory fibers are recruited. Paired-pulse ratio (PPR) is a technique that assesses the neural activity within SI by delivering doublets of electrical nerve stimuli with a short interstimulus interval (i.e., 10-30 ms). The resulting N20-P25 generated by the second stimulus (i.e., SEP 2) is suppressed relative to the first N20-P25 (i.e., SEP 1). The ratio of SEP 2 to SEP 1 decreases when median nerve stimulation intensity increases within a range from sensory threshold (ST) to 1.2x motor threshold (MT) for a twitch in the abductor pollicis brevis (APB) [20]. PPR is potentially a powerful tool for studying intracortical SI mechanisms, yet there remain several unanswered questions that currently limit its usage. First, the relationship between PPR and the magnitude of the afferent volley remains unclear. Since SEPs are saturated at ~ 50% of $SNAP_{max}$, one would predict that PPR would also be saturated if its magnitude is determined primarily by the afferent volley. Decreases in PPR are, however, mediated by increases or decreases in SEP 1 and SEP 2, respectively. Therefore, when assessing SI intracortical measures it is important to evaluate both PPR and SEP 2 as a function of intensity to fully understand these relationships.

SAI is a measurement assessing the inhibitory influence of the afferent volley on neural circuits within M1. SAI is evoked by pairing a peripheral nerve stimulus with a subsequent Transcranial magnetic stimulation (TMS) pulse over M1. When nerve stimulation precedes TMS at short latencies after the N20 (i.e., 2 to 8 ms) the resulting motor evoked potential (MEP) generated from TMS is suppressed [1]. Importantly, SAI

increases (i.e., increased inhibition) when median nerve stimulation increases from ST to MT [26]. The relationship between SAI and the afferent volley, however, remains unknown. SAI may be mediated by transmission of the afferent volley via SI or via direct thalmocortical projections to M1. Therefore, if SAI were mediated by transmission through SI one would expect SAI to follow a similar recruitment pattern to both SEPs and PPR.

The present study investigated the relationship between the magnitude of the median nerve afferent volley based on percentages of $SNAP_{max}$ with SEPs, PPR and SAI. Through correlation analyses, the relationships between these measures were also explored. Based on Gandevia and Burke (1984) it was hypothesized that SEPs would saturate at ~ 50% $SNAP_{max}$ [46]. Further, it was hypothesized that PPR and SAI would follow a similar recruitment pattern and also saturate at ~ 50% $SNAP_{max}$. Results indicate that SEPs and SAI increase and PPR decreases to ~ 47% $SNAP_{max}$ with no change thereafter. Further, correlations reveal that SNAPs were correlated with SEPs but not SAI, while SAI is correlated with PPR and SEPs. This supports the hypothesis that the afferent volley arrives in M1 via SI and not due to direct thalamocortical synapses.

4.2 Methods

Participants

Twenty-three right-handed individuals were studied (10 males; mean age: 23 ± 1.5). Participants were determined to be right handed by the Edinburgh Handedness Scale [109]. The study conformed to the declaration of Helsinki and was approved by the McMaster Research and Ethics Board. All individuals provided written consent prior to participation.

SNAPs, nerve stimulation & SEPs

SNAPs were recorded over the median nerve (MN) at the elbow just proximal to the medial epicondyle. The MN, a mixed nerve containing both sensory and motor fibers, was stimulated using a bar electrode at the wrist slightly medial and proximal to the styloid process of the radius and just lateral to the tendons of the wrist. Five median nerve stimulation intensities were used and defined as the stimulator output that elicited ~ 25%, 50% and 75% of $SNAP_{max}$ and 1.2 x and 2.4 x MT based on a visible muscle twitch in the (APB). Percentages of $SNAP_{max}$ were determined before collections of SEPs and SAI by averaging the SNAP over 40 sweeps and the stimulator was adjusted until the amplitude of the SNAP approximated the intended percentage value for each participant.

SEPs were acquired at electrode position C3' and referenced to Fz based on the International 10-20 system with the ground electrode over the clavicle. Impedance was < 5 kΩ at each scalp electrode. For each intensity tested, 500 pairs of median nerve stimuli were delivered and separated by an interstimulus interval (ISI) of 30 ms [110-112]. Pairs

were delivered at a frequency of 1 Hz. The peak-to-peak N20-P25 response that followed the first stimulus was defined as SEP 1 and the peak-to-peak N20-P25 response that followed the second stimulus was defined as SEP 2. SEP signals were amplified (10K), band pass filtered (high pass of 2 Hz and low pass of 2500 Hz), collected (CED 1401, Signal v5) and stored on a personal computer for offline analysis.

Short-latency afferent inhibition (SAI)

EMG was recorded with Ag – AgCl surface electrodes (9 mm) placed over the FCR muscle of the right forearm with the active electrode placed ~ 3 cm distal and 2 cm lateral to the medial epicondyle, the reference was placed over the tendons of the wrist and the ground electrode placed over the medial styloid process of the wrist. EMG signals were amplified (x 1000), band pass filtered (high pass of 20 Hz and low pass of 2500 Hz) and collected (CED 1401, Signal v5) for offline analysis. TMS was performed using a 50 mm inner diameter figure-of-eight branding coil connected to a Magstim 200^2 stimulator (Magstim, UK). The motor hotspot for FCR was determined as the location providing the most reproducible MEP in the relaxed FCR muscle. The coil was positioned 45 degrees to the mid-sagittal line to induce a current in a posterior-to-anterior direction over the left-hemisphere motor cortex. Resting motor threshold (RMT) was tested at the motor hotspot and defined as the lowest stimulator intensity to elicit MEPs of ≥ 50 μV in 5 out of 10 consecutive trials [57]. Brainsight Neuronavigation (Rogue Research, Canada) was used to target and track the TMS coil position and orientation corresponding to the location of the motor hotspot. To elicit SAI, the TMS intensity was set to evoke MEPs of ~ 1 mV in the relaxed FCR. The ISI between the peripheral nerve stimulus and TMS

pulse was derived from the latency of the N20 component in each participant and an additional 2 ms was added to elicit greatest inhibition [1]. SAI was tested at intensities defined by the $SNAP_{max}$ (i.e., 25%, 50% and 75%) and at 1.2 x and 2.4 x MT. Each of the afferent volley intensities was tested in a separate block of 30 trials; fifteen conditioned MEPs (i.e., $MEP_{nerve\text{-}TMS}$) randomly presented with fifteen unconditioned MEPs (i.e., MEP_{TMS}). A 5-second inter-trial-interval was used.

Experimental Protocol

Participants were subject to five testing blocks, corresponding to each stimulation intensity. Within each block SNAPs, SEPs, PPR and SAI were collected at a single afferent volley intensity. The order of intensities collected was pseudo-randomized across participants using a William's square design. During the first intensity block SEPs were always collected first to calculate the N20 latency, a latency required to determine the ISI for SAI. The subsequent blocks were randomized for the order in which dependent measures were collected.

Data Analyses

The actual SNAP amplitudes (i.e., actual SNAPs attained: 20%, 44%, 49%, 71% and 100% $SNAP_{max}$) acquired during testing were analyzed for each of the five intensities tested. Subsequently we compared the amplitude of the actual SNAPs between neighboring intensities (i.e., actual data: 20% vs 44%; 44% vs 49%; 49% vs 71%; and 71% vs 100% $SNAP_{max}$) via paired two-tailed *t*-tests to ensure levels can be treated as separate intensities. SNAPs that were not significantly different from their neighboring

SNAP intensities were averaged to create a single intensity. In this instance all dependent measures were averaged across these two intensities. SEPs were averaged over the 500 epochs. Intracortical inhibition within SI was determined by the amplitude of SEP 2, which is suppressed at ISIs of 30 ms [110-112]. PPR was measured as the ratio of SEP 2 divided by SEP 1. SAI was expressed as the absolute amplitude of the conditioned MEPs (i.e., $MEP_{nerve\text{-}TMS}$) and compared to the unconditioned MEP (i.e., MEP_{TMS}).

The amplitude of SEP 1, SEP 2, PPR and SAI were subject to one-way repeated measures ANOVA with factor INTENSITY (4 levels corresponding to the actual SNAPs recorded during testing: 20%, 47%, 71%, 100% $SNAP_{max}$). Upon significance, post-hoc Tukey's HSD test was used. For SAI, to ensure the unconditioned MEP (MEP_{TMS}) was not different between intensities a one-way repeated measure ANOVA with factor INTENSITY (4 levels: 20%, 47%, 71%, 100% $SNAP_{max}$) was used. To test the hypothesis that both PPR and SAI should increase to 47% $SNAP_{max}$ (~ 50% $SNAP_{max}$) [20,26] a one-tailed paired t-test compared the respective measures at 20% versus 47% $SNAP_{max}$. Saturation within SEPs, PPR and SAI was determined by the percentage of afferent volley at which measures cease to statistically increase. Pearson's correlation analyses were performed between SNAPs, SEPs, PPR and SAI to assess the relationship between SNAPs and responses by accounting for individuals actual SNAP values. Significance was set at $p < 0.05$ and if the assumptions of sphericity were not met, Greenhouse-Geisser corrections were used.

4.3 Results

Twenty-three right-handed individuals were studied (10 males; mean age: 23 ± 1.5). One participant was not able to complete the highest intensity due to discomfort, and one participant had abnormal SEP responses as determined as greater than 2-SD away from the mean at all intensities. Therefore, data from 21 individuals (8 males; mean age: 23 ± 1.54) were included in all subsequent analyses.

SNAPs

Median nerve stimulation was delivered to obtain SNAPs of approximately 25%, 50% and 75% $SNAP_{max}$ and at 1.2 x and 2.4 x MT. The actual group-averaged nerve intensities delivered, based on the percentage of $SNAP_{max}$ in each participant are shown in Table 1 are referred to herein. As can be seen in Table 1, 1.2 x MT evoked ~ 50% $SNAP_{max}$ while 2.4 x MT equated to ~ 100%. MT in mA fell between the 20% and 44% $SNAP_{max}$ (i.e., 10.57 mA). SNAPs were not significantly different between 44% $SNAP_{max}$ and 1.2 x MT (49% $SNAP_{max}$) ($p=0.106$) and data for these two intensities were averaged for each individual prior to subsequent analyses. Following this average, all adjacent intervals of % $SNAP_{max}$ were statistically different (20% vs 47% $p < 0.001$, 47% vs 71% $p < 0.001$, 71% vs 100% $p < 0.001$).

SEPs

Figure 1A displays the group-averaged peak-to-peak N20-P25 amplitude as a function of the percentage of $SNAP_{max}$. One-way ANOVA revealed a significant effect of INTENSITY ($F_{(2.07,41.48)}=16.41$; $p<0.001$) and post-hoc Tukey's revealed greater N20-

P25 amplitudes at 47%, 71% and 100% versus 20% $SNAP_{max}$. The maximum amplitude of the N20-P25 occurred at 71% $SNAP_{max}$, but, statistically, SEPs did not increase beyond the amplitude obtained at 47% $SNAP_{max}$. Figure 1B illustrates an example SEP dataset from one individual at each percentage of $SNAP_{max}$.

The group-averaged PPR is shown in Figure 1C and revealed a significant effect of INTENSITY ($F_{(3,60)}$=3.698; p=0.016). Compared to 20% $SNAP_{max}$ PPR was reduced at 47% in support of the hypothesis (one-tailed $p = 0.005$) and 71% ($p < 0.05$). Statistically PPR did not change beyond 47% and was therefore saturated at this intensity. However, as is shown in Figure 1D reductions in PPR are not mediated by decreases in the amplitude of SEP 2 (SEP 2; INTENSITY, $F_{(3,60)}$=1.118; p=0.349) but instead relate to increases in SEP 1. Further, SEP 2 had a maximum amplitude of ~ 2 μV at all intensities and suggests a potential ceiling effect for activation within SI after a nerve stimulus 30 ms prior.

SAI

Figure 1E plots the group-averaged data for the test MEP (i.e. MEP_{TMS}) and the conditioned MEP (i.e. $MEP_{nerve\text{-}TMS}$) at each percentage of $SNAP_{max}$. One-way ANOVA revealed a significant effect of INTENSITY ($F_{(4,80)} = 6.31$; $p < 0.001$) indicating the presence of SAI at 47%, 71% and 100% of $SNAP_{max}$ ($p < 0.05$, post-hoc Dunnet's test; TS versus each CS-TS). The unconditioned MEP amplitude was not different across the afferent volley intensities ($F_{(3,60)} = 0.255$, $p = 0.857$). Further, in support of the hypothesis, SAI increased from 20% to 47% $SNAP_{max}$ (p=0.0249) the maximum depth

observed. Figure 1F illustrates an example SAI dataset from one individual at each percentage of $SNAP_{max}$ obtained in this individual.

Correlation Analyses

Correlation analyses between SNAPs, SEPs, PPR and SAI are shown in Figure 2. SNAPs are significantly correlated with SEPs (Figure 2A) ($r = 0.216$, $p = 0.024$) and PPR (Figure 2B) ($r = 0.228$, $p = 0.019$) but are not correlated with SAI (Figure 2C) ($r = 0.033$, $p = 0.382$). These correlation analyses show that across all intensities SNAPs are significantly related to excitation within SI and are not predictors of inhibition within M1. SAI and SEP 1 (Figure 2D) are positively correlated ($r = 0.276$, $p = 0.006$) indicating that an increase in SEP 1 amplitude relates to increased SAI. SAI and PPR (Figure 2E) are positively correlated ($r = 0.221$, $p = 0.022$) such that decreasing PPR (i.e., towards a value of 1 in Figure 2E) reflects a concomitant increase in SAI.

Additionally, to represent trends seen in changes to SEPs, PPR and SAI with increases in $SNAP_{max}$ second order polynomial trend lines are shown in Figure 2F. Together these results indicate that as the percentage of $SNAP_{max}$ increases SEPs, PPR and SAI respond similarly to one another and saturate at the same % $SNAP_{max}$.

4.4 Discussion

The present study investigated the stimulus-response relationship between median nerve SNAPs and SEPs, PPR and SAI. Several novel findings were revealed. All measures plateaued at ~ 50% of $SNAP_{max}$, and this intensity is thought to correspond to the

maximum recruitment of sensory fibers in the median nerve [38,46]. Second, median nerve stimulation intensity above 20% and below 47% $SNAP_{max}$ should, based on our sample size, allow for all measures to adequately flux, and is ideal for intervention studies that aim to increase or decrease SEPs, PPR and SAI. Last, intracortical SI measures are correlated with M1 intracortical inhibition, supporting the notion that SAI circuitry involves synaptic projections from SI to M1. We discuss these findings and the implications from our work.

The amplitude of the N20-P25 SEP increased up to ~ 50% $SNAP_{max}$ (i.e. 1.2 x MT) and plateaued beyond this point, similar to previous research [38,46]. The N20 and P25 components of the SEP are generated by pyramidal neurons in micro and macro columns of area 3b [24,113] that receive their excitatory input from spiny stellate cells [18]. Increasing the strength of this excitation via changes in the afferent volley is reflected in the pyramidal cell population response [114-116] and is likely to cause the observed increase in SEP amplitude [117,118]. In support of previous literature [46], our data suggests that excitation of SI increases with gains in the afferent volley and the plateau likely reflects the point at which all sensory fibers within the median nerve have been recruited (i.e. ~ 50% $SNAP_{max}$).

Similar to SEPs, PPR saturates at ~ 50% $SNAP_{max}$. Previous reports have shown a decrease in PPR to 1.2 x MT [20]. Our data support their finding and also indicates that PPR is saturated at this intensity. The measure of PPR is calculated by the ratio of SEP 2 to SEP 1 and is itself comprised of both excitation within SI (SEP 1) and inhibition of excitation within SI (SEP 2). The mechanism of SEP 2 suppression relative to SEP 1, is

thought to proceed by GABAergic neurotransmission [20,51] whereby activated pyramidal cells excite inhibitory parvalbumin (PV) expressing interneurons [21], likely double bouquet cells [22], that via recurrent inhibition, act to inhibit the pyramidal cells themselves [21,22]. Therefore, the response to the second nerve stimulus is suppressed relative to the first. However, one important observation is that the amplitude of SEP 2 is not altered by changes in the afferent volley. Therefore the magnitude of recurrent inhibition is largely unchanged by increases in intensity and the decreases in PPR are largely driven by increases in the initial excitation of pyramidal neurons. These data highlight the need to consider the interpretation of PPR; changes in PPR do not necessarily reflect changes in inhibition but rather, as we show, changes in initial excitation of SI. The available literature in animal models suggests that the amplitude of SEP 2 better isolates the contribution of recurrent inhibition [21]. We note that SEP 2, is not only insensitive to changes in the afferent volley but also appears to not exceed ~ 2 uV. In our data, the decrease in PPR (Figure 1C) is driven by increased SEP 1 and is most accurately interpreted as an increase in SI excitation.

SAI increased up to 50% $SNAP_{max}$, following closely with changes in SEP 1 and PPR. These data support the finding that SAI increases from ST to MT which is only slightly below our 50% $SNAP_{max}$ [26]. SAI is a cortically mediated circuit implicated in motor control [3,27,28] with the afferent volley inhibiting the late I-wave generating neurons within M1 as shown by reductions in the amplitude of descending I-3 waves in epidural recordings [29]. It is proposed that I-waves are generated by excitatory cells within in layers 2/3 and layer 5 which synapse onto GABAergic neurons that in turn offer recurrent

inhibition [30]. Increases in SAI with an increase in afferent volley may occur via increased excitation of these GABAergic interneurons that synapse on the late I-wave generating neurons resulting in an increase in inhibition on the late I-waves and reduced MEP amplitude.

The pathway by which the afferent volley projects to M1 to produce SAI remains unclear (i.e. thalamo-cortical to M1 [30] or relay through SI). Although our data cannot exclude a direct thalamo-cortical route for the SAI circuit, our results support a relay through SI. Correlations between the SNAP amplitude and measures of SEPs, PPR and SAI support the mechanisms provided above. SNAPs are significantly correlated with SEPs ($p = 0.024$) and PPR ($p = 0.019$) but are not correlated with SAI ($p = 0.382$). Our finding of SNAPs not being correlated with SAI support our notion that SAI is evoked by the afferent volley projecting through SI to M1 rather than via direct connections to M1. If SAI was evoked via direct projections to M1 we would expect a significant correlation of SNAPs with SAI, but this is not the case and SAI is correlated with intracortical measures within SI. Therefore, our data support the theory for an SI relay in the afferent conditioning of M1. One mechanism to explain such conditioning involves pyramidal cells within SI that have long-range horizontal monosynaptic excitatory projections to neurons within M1 [31] and are able to drive the output of cells in the upper layers of M1 but have little influence on the cells in the lower layers [31,32]. The early I-1 wave is generated by TMS stimulation of neurons in layers 2/3 that have monosynaptic connections to neurons within layers 5 and together form a canonical circuit where GABAergic inhibitory neurons act through recurrent inhibition on these cells to suppress

each subsequent I-wave [30]. SAI is associated with a reduction in the amplitude of the late I-3 wave but not the earlier I-waves [29] and the GABAergic inhibitory neurons are involved in the generation and suppression of late I-waves and not early [30]. Therefore, we suggest long-range horizontal projections from SI pyramidal cells may excite these GABAergic inhibitory cells thereby increasing the recurrent inhibition on the late I-waves resulting in SAI. Increasing the excitation of SI pyramidal cells with a larger afferent volley (and greater SEP amplitude) potentiates the GABAergic inhibitory cells and increases the depth of SAI.

Saturation Points and Implications on Future and Past Research

This research demonstrates that stimulus-response patterns of SEP 1 and PPR are very similar to that observed in SAI, suggesting common neural mechanisms that mediate these circuits. As shown in Figure 2F, all three measures are recruited similarly at low intensities and either saturate or begin to saturate at ~ 50% $SNAP_{max}$. Statistically, all measures saturate at ~ 50% $SNAP_{max}$. One explanation for saturation is that all sensory fibers are recruited by ~ 50% of $SNAP_{max}$ as described elsewhere [38]. Alternatively, subcortical structures including the dorsal column nuclei, ventro-posterior lateral/anterior nuclei of the thalamus and thalamic reticular nucleus may provide a gating mechanism to reduce the afferent information arriving at the cortex [19].

Irrespective of the mechanism that mediates saturation of SAI, SEP and PPR, these data have important implications for basic and clinical neuroscience research. We first must consider the advantages of finding the point of saturation. The saturation point localizes

the upper limit for the sensitive part of the recruitment curve, that is, the part of the curve that is subject to change with changes in the intensity. Understanding the upper and lower limits of the stimulus-response relationships for SEPs, PPR and SAI is important for research aiming to alter these measures (SAI [33-35] PPR [34,35] and SEPs [35-37]). We also note that motor threshold for a twitch in APB is observed at a current slightly below that to achieve ~ 50% $SNAP_{max}$. Therefore, stimulation intensities set above motor threshold are likely to lead to saturation in these measures and may limit opportunities to observe increases in their magnitude. Our data suggests that, for studies aiming to alter these measures, median nerve stimulation should be delivered at intensities below motor threshold, above 20% and below 40% of the $SNAP_{max}$ to allow for growth and decline of the measured response.

Limitations

In our experiment we studied a relatively young and healthy adult population. It is not known whether such stimulus-response functions will be observed in elderly and/or special populations. Additionally, our work investigated the recruitment curves for median nerve stimulation and it is not known if these results will apply to other nerves tested.

4.5 Conclusions

Our data shows that SEPs, SAI and PPR have similar recruitment profiles. These data support the hypothesis that the afferent volley is important in determining the depth of SI cortical excitation (SEPs, PPR) and inhibition within M1 (SAI) and that neural activity within SI are significant predictors of changes in M1. Further, we indicate that measures of intracortical inhibition within SI defined by SEP 2 do not change as a function of intensity and that decreases in PPR with intensity is driven by increases in SI activation. Last, this work provides evidence of an effective method to define nerve intensities for plasticity protocols aimed at altering SEPs, PPR and SAI physiology.

4.6 Table 2: Percent Afferent Volley

Intended	25% SNAP	50% SNAP	1.2 x MT	75% SNAP	2.4 x MT
Actual (%)	20%	44%	49%	71%	100%
SD	10.2	15.3	23.6	19.7	0.00
			47%		
Actual (mA)	9.16	11.82	12.64	15.05	24.88
SD	3.77	4.40	4.23	5.27	8.48

Figure 7:

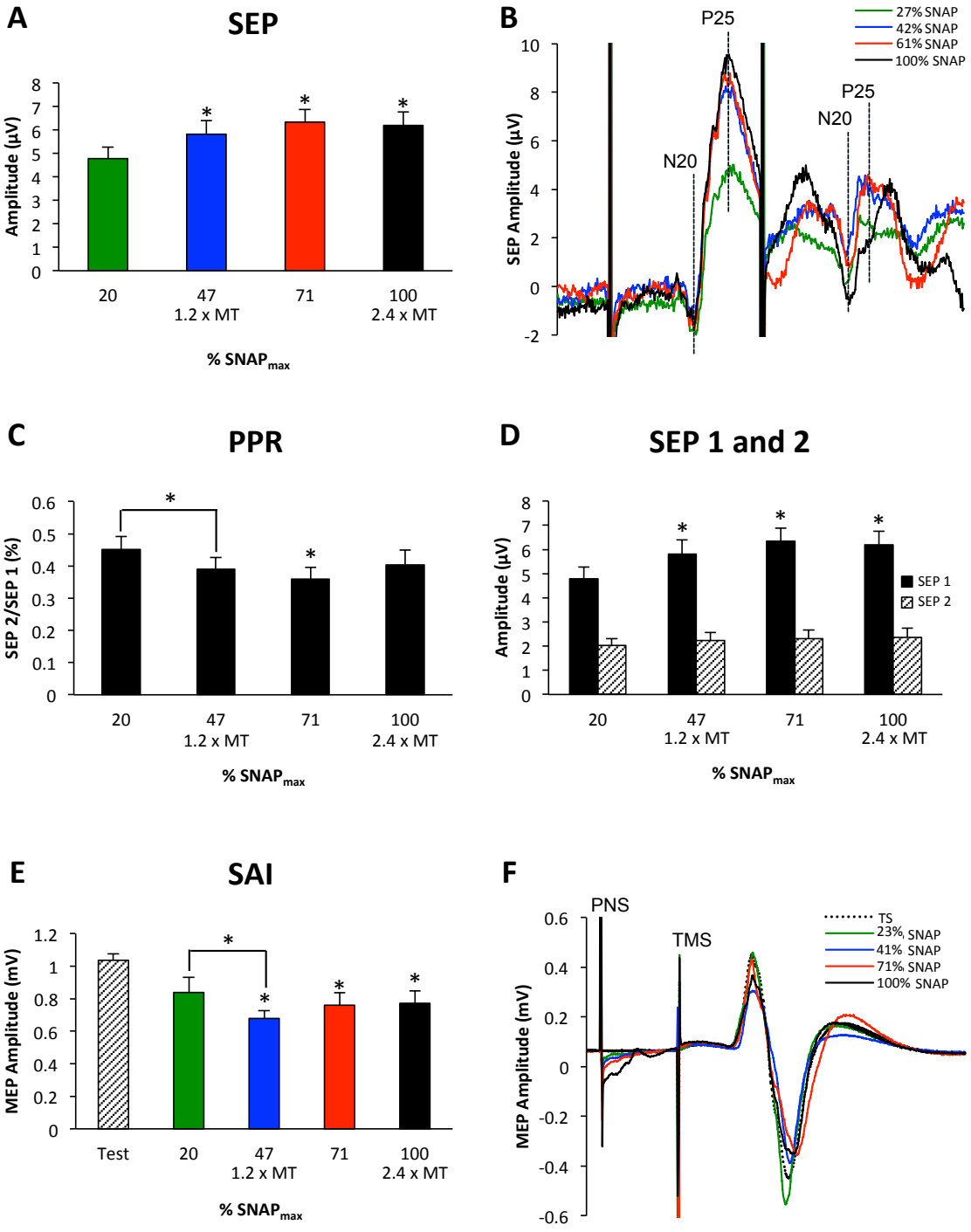
A
SEP
Amplitude (μV)
20
47
1.2 x MT
71
100
2.4 x MT
% SNAPmax
B
P25
N20
P25
N20
27% SNAP
42% SNAP
61% SNAP
100% SNAP
SEP Amplitude (μV)
C
PPR
SEP 2/SEP 1 (%)
% SNAPmax
D
SEP 1 and 2
Amplitude (μV)
SEP 1
SEP 2
% SNAPmax
E
SAI
MEP Amplitude (mV)
Test
% SNAPmax
F
PNS
TMS
TS
23% SNAP
41% SNAP
71% SNAP
100% SNAP
MEP Amplitude (mV)

Figure 8:

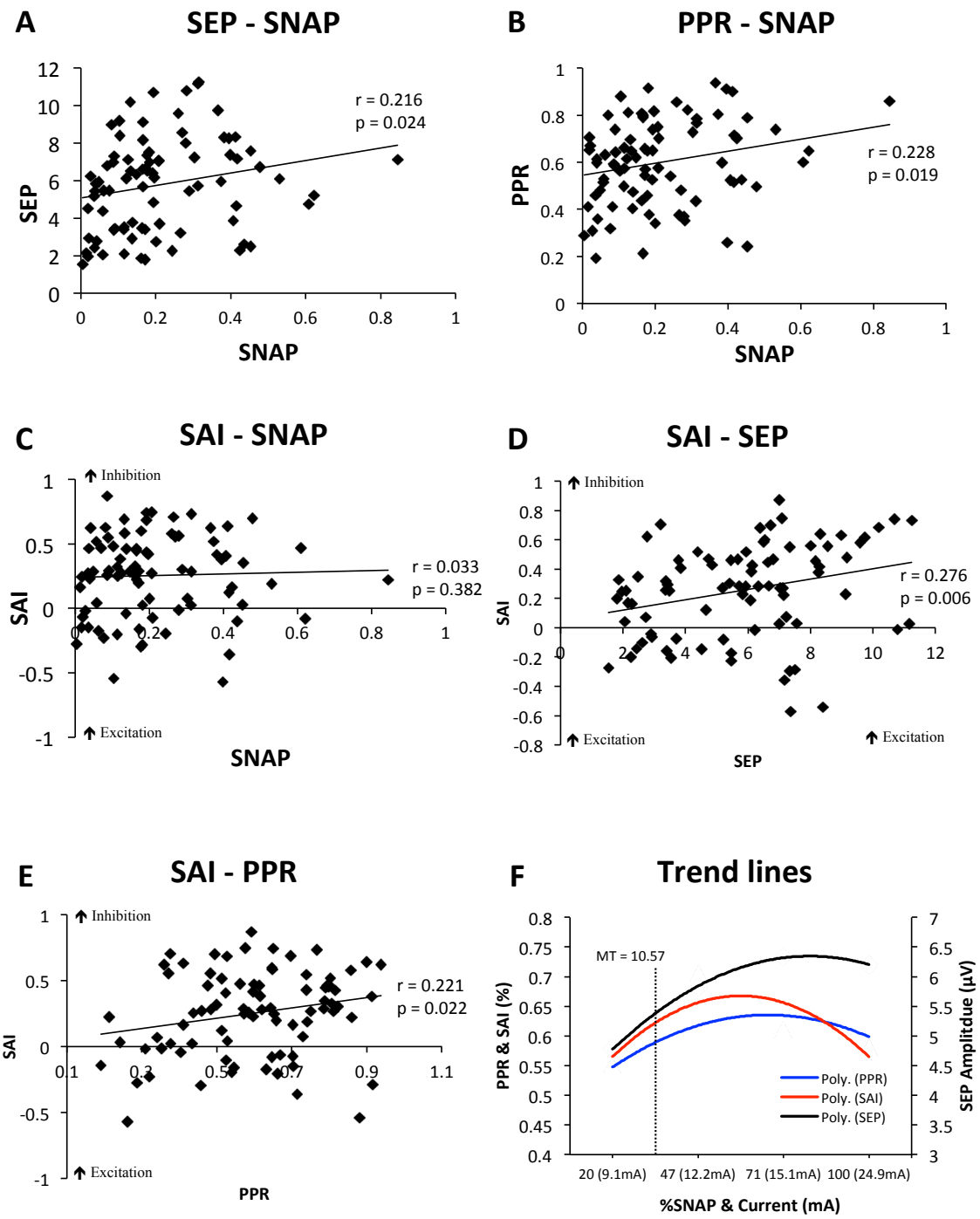
A
SEP - SNAP
r = 0.216
p = 0.024
SEP
SNAP
B
PPR - SNAP
r = 0.228
p = 0.019
PPR
SNAP
C
SAI - SNAP
Inhibition
Excitation
r = 0.033
p = 0.382
SAI
SNAP
D
SAI - SEP
Inhibition
Excitation
Excitation
r = 0.276
p = 0.006
SAI
SEP
E
SAI - PPR
Inhibition
Excitation
r = 0.221
p = 0.022
SAI
PPR
F
Trend lines
MT = 10.57
Poly. (PPR)
Poly. (SAI)
Poly. (SEP)
PPR & SAI (%)
SEP Amplitdue (µV)
20 (9.1mA)
47 (12.2mA)
71 (15.1mA)
100 (24.9mA)
%SNAP & Current (mA)

Figure Legends

Figure 7: Somatosensory Function

A) Group averaged recruitment curve of N20-P25 (with standard error bars) as a function of increasing percentage of actual $SNAP_{max}$ recorded. Compared to 20%, SEPs increase in amplitude at 47%, 71% and 100% with no differences from 47% to 100% $SNAP_{max}$. **B**) Individual SEP traces depicting N20-P25 amplitude of SEP 1 and SEP 2. Traces are color coded to reflect data in Figure 1A. Actual percentages of $SNAP_{max}$ are shown in the figure legend for this participant. **C**) Group averaged PPR of the SEP 2 to SEP 1. Data shows a significant decrease in PPR between 20% and 71% $SNAP_{max,}$ as indicated by the asterisk over the bars and *a-priori* testing shows a significant decrease in PPR from 20% to 47% $SNAP_{max}$ depicted by asterisks between the bars. **D**) Group averaged SEP 1 and SEP 2 amplitudes as a function of the percent $SNAP_{max}$. Black bars represent SEP 1 and reflects data shown in Figure 1A, while hatched bars reflect the amplitude of the SEP 2. SEP 2 does not alter with changes in the afferent volley. **E**) Group averaged unconditioned and conditioned MEP data at each percentage of $SNAP_{max}$ representing SAI. Asterisks over the bars indicate significant reduction in the conditioned MEP amplitude compared to the unconditioned MEP amplitude (47%, 71% and 100% $SNAP_{max}$) while asterisks between the bars represents *a-priori* testing that show significant increases in SAI from 20% to 47% $SNAP_{max}$. **F**) Individual MEP traces depicting the unconditioned MEP (MEP_{TMS}) and the conditioned MEP ($MEP_{nerve\text{-}TMS}$) at each of the afferent volley intensities. Actual % $SNAP_{max}$ are shown in the figure

legend for this participant.

Figure 8: Correlation Analyses

A) Correlations between SNAP and SEP 1 reveal a significant positive correlation showing that as SNAP increase the excitation in SI increases. **B)** Correlations between SNAP and PPR reveal a significant positive correlation showing that as SNAP increases the ratio decreases (x-axis proceeds towards 1). **C)** Correlations between SNAP and SAI reveal no correlation and show that the afferent volley is not significantly related to the inhibition within M1. **D)** Correlations between SAI and SEP 1 reveal a significant positive correlation showing that as SEP increase the depth of SAI increases. **E**) Correlations between SAI and PPR reveal a significant positive relationship. As the ratio of SEP 2/SEP 1 reduces the inhibition within M1 increases as well. **F**) Second order polynomial trend lines of the recruitment curves for each measurement are shown in order to represent how each measure responds to the increases in SNAP. Represented on the graph is our measurement of MT and where this intensity would lie on the recruitment curves. As indicated MT lies slightly below the saturation point and may not allow for increases in these measures to occur. Additionally, visually all three measures show the saturation occurring at ~ 50% of the $SNAP_{max}$.

Chapter 5: General Discussion

5.1 Summary of Experiments

This Master's thesis examined alterations to sensorimotor integration in individuals with chronic cervical spinal cord injury through measures of MEPs, SNAPs, SEPs and SAI. Two experiments were conducted to investigate a) whether individuals with spinal cord injury show alterations in these measures and b) whether alterations in these measures are likely to be explained by alterations in the afferent volley. This thesis is the first attempt to examine alterations in the upper limb sensorimotor pathways in individuals with chronic cervical spinal cord injury and investigate the relationships between SEPs, PPR, SAI and the afferent volley as well as their interrelatedness. Results from the first experiment show that several alterations exist within the sensorimotor system in individuals with chronic spinal cord injury. First, the MEP amplitude and MTs are reduced and increased, respectively in the active state and not the resting state. Second, SNAPs are reduced in individuals with SCI while SEPs are not reduced. Finally, SAI, which measures sensorimotor integration, is reduced in individuals with SCI in both the active and resting states. The second experiment, which sought to investigate what the relationship between the afferent volley and measures of somatosensory function, found that all measurements of SEPs, PPR and SAI increase with the afferent volley and all saturate at the same intensity. Results from both experiments provide novel information regarding sensorimotor function in the upper limbs in individuals with spinal cord injury and how these measure function as the afferent volley arriving in the cortex increases.

The following sections will discuss possible mechanisms, the impact of the experiments and the limitations and future directions of the work.

5.2 Neural models and mechanisms

For my dissertation, I have created a neural model (Figures 9-12) to assist in the explanation and integration of the data and will refer to these figures for the remainder of the discussion. Specifically, models are provided to explain the responses of M1 and SI to a TMS pulse and nerve stimulus respectively, how SAI is evoked, the effect of altering the afferent volley and how neural pathways are likely to be affected in individuals with spinal cord injury.

Neural model describing mechanisms of MEPs, SEPs and PPR

The proposed neural model describing the mechanisms behind generation of MEPs, SEPs and PPR is shown in Figure 9. The afferent volleys travel to somatosensory cortex via relay through the VPL of the thalamus and synapse onto spiny stellate (SS) cells within layers 5 of SI [17,42] [14,18]. These SS have excitatory synapses with pyramidal cells in layers IV and V of SI. The excitation of these pyramidal cells and their excitation of other pyramidal cells in neighboring cortical columns give rise to the N20-P25 SEP. The pyramidal cells also have excitatory synapses with PV expressing inhibitory interneurons that are likely to be DB cells [21]. Once activated, these cells synapse back with the pyramidal cell and provide recurrent inhibition. Therefore, the next excitatory synapse

onto the pyramidal cell from the SS cell will be reduced since the PV cells are actively inhibiting the pyramidal cell giving us the suppressed second N20-P25.

TMS when delivered in the PA orientation preferentially excites superficial pyramidal cells within layers 2/3 of M1 [56]. These pyramidal cells have excitatory synapses with other pyramidal cells in layer 5 of M1, which once activated send a descending volley down the spinal cord termed the I-1 wave. Pyramidal cells within layers 2/3 and 5 have excitatory connections with GABAergic neurons that then through inhibitory synapses create recurrent inhibition on the pyramidal cells [30]. The layer 5 pyramidal cells also have excitatory synapses back with the pyramidal cells in layer 2/3. Therefore, after the initial excitation of the pyramidal cell via TMS the pyramidal cells in layer 2/3 are re-excited by the cells in layer 5, to a lesser extend due to the GABAergic inhibition, and in turn synapse again with the pyramidal cells in layer 5 and with the GABAergic inhibitory cells. This circuit is repeated continuously leading to the generation of the late I-waves [30]. Summation of the I-waves at the alpha motor neuron leads to the generation of an action potential resulting in a motor evoked potential or muscle twitch within the muscle of interest. The continual reciprocal activation of cells in layer 2/3 and 5 supports the periodicity of the I-waves (1.5 ms each) [30] and the GABAergic inhibition supports the finding that $GABA_A$ agonists reduce the amplitude of the MEP as the late I-waves would be suppressed to a greater extent [62].

Neural model describing mechanisms of SAI

The proposed neural model describing how SAI is generated is depicted in Figure 10. The pathway of afferent transmission from the afferent volley to M1 is debated for the

circuit of SAI. It may traverse a path through SI or be directly projected to M1 via thalamocortical connections. These data support the hypothesis that the somatosensory afferent volley first travels through SI. Literature in animal models demonstrates an excitatory projection between SI and M1 such that stimulation of SI leads to the generation of EPSPs within M1. These responses are dose dependent and increasing the stimulation of SI leads to greater EPSPs evoked in M1 [31]. The finding that SAI is not significantly correlated with the amplitude of SNAP refutes the hypothesis that afferents arrive to M1 via direct thalamocortical connections and the finding that SAI is correlated with SEPs and PPR supports the hypothesis that afferents first travel through SI and these excitatory connections are likely the pathways used to evoke SAI. In my model I suggest SI projects and synapses onto the GABAergic neurons responsible for generating I-waves. Excitation of these cells result in greater inhibition of the late I-waves [29] resulting in SAI.

Neural model describing mechanisms of increasing afferent intensity

The proposed neural model describing changes in measures of SEPs, PPR and SAI with increased afferent intensity is shown in Figure 11. The volume of activation within SI is increased as shown by increases in SEP 1. Greater activation within SI would lead to increased output of the pyramidal cell to M1 [31] and greater excitation of the GABAergic neurons resulting in increased depth of SAI. However, increasing the activation of SI does not lead to decreases in the amplitude of SEP 2 suggesting that the input onto the PV expressing inhibitory neurons is either unaffected or the inhibitory output provided by these PV cells does not change with increases in the afferent volley

and provides a constant inhibitory influence on that pyramidal cells providing a ceiling to the amount they can be activated after a prior nerve stimulation.

Neural model describing mechanisms behind alterations in MEPs, and SAI with SCI

The proposed model to describe the changes that occur in measures of MEPs and SAI is depicted in Figure 12. Data in individuals with spinal cord injury show reduced SNAPs, MEPs and SAI but show normal SEP amplitudes. The median nerve is a mixed nerve containing both afferent and efferent fibers. Since, participants show normal SEPs and altered MEPs it is likely that majority of my cohort experience a greater amount of damage to the motor fibers as opposed to the sensory fibers. Further, the data support that reductions in SAI are not mediated by decreased activation of SI resulting from reduced afferent volley since both SCI group and control group show similar activation of SI. Therefore in these two groups the excitation of GABAergic cells within M1 should be similar resulting in similar depths of SAI. SAI is however, reduced in the SCI group, likely to be resulting from either changes in the synapse from SI to M1 resulting in reduced activation of GABAergic neurons or alternatively, aberrations exist within the GABAergic neurons themselves. It is known that late I-waves, which are affected by these GABAergic neurons, are altered in individuals with SCI [119,120] supporting this hypothesis that the function of these cells is impaired in individuals with spinal cord injury.

Figure 9: Mechanisms in motor and somatosensory cortices

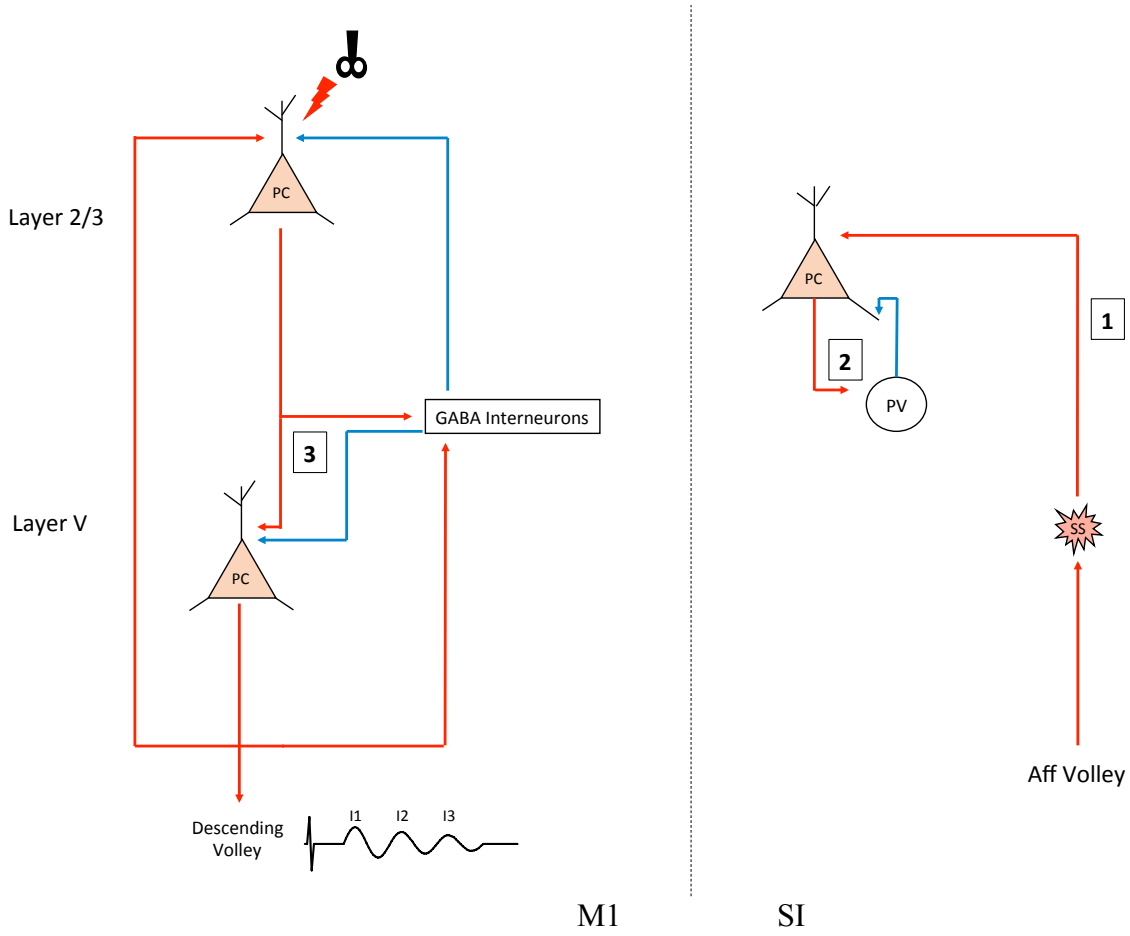

Figure 10: Mechanisms behind short-latency afferent inhibition

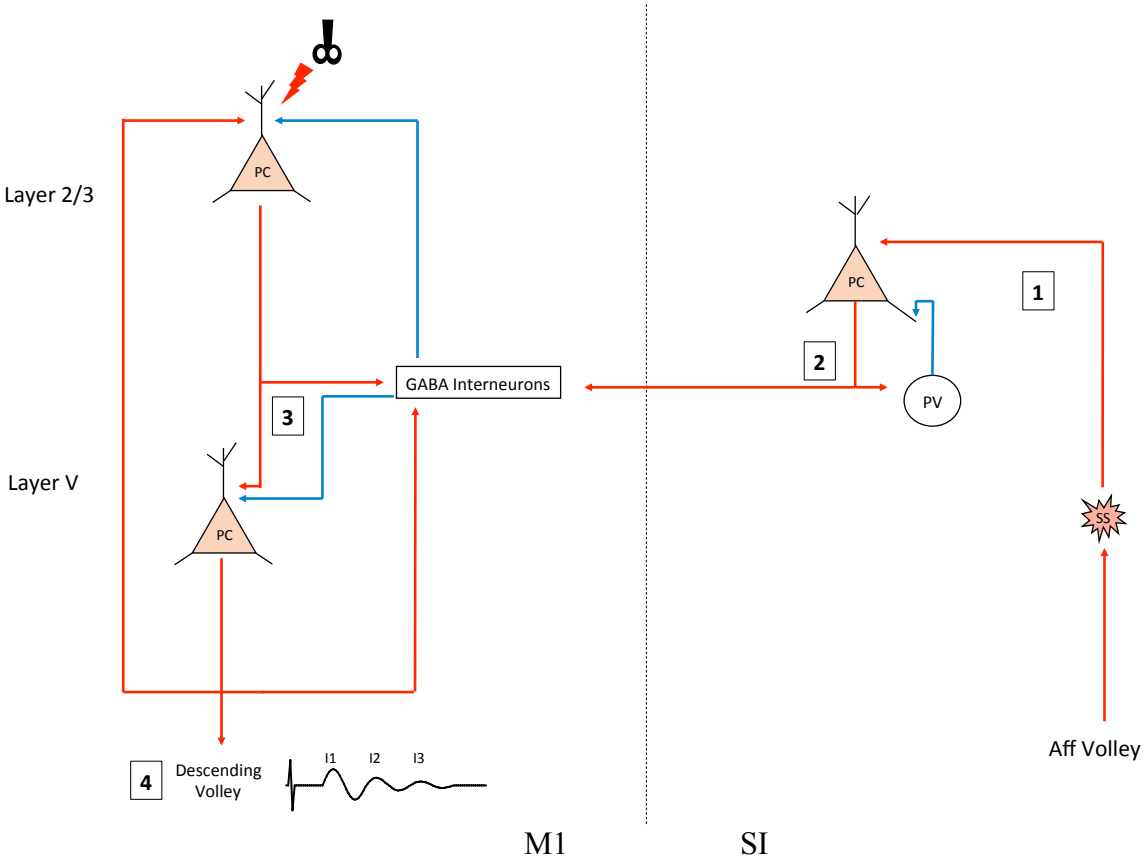

Figure 11: Mechanisms behind changing afferent intensity

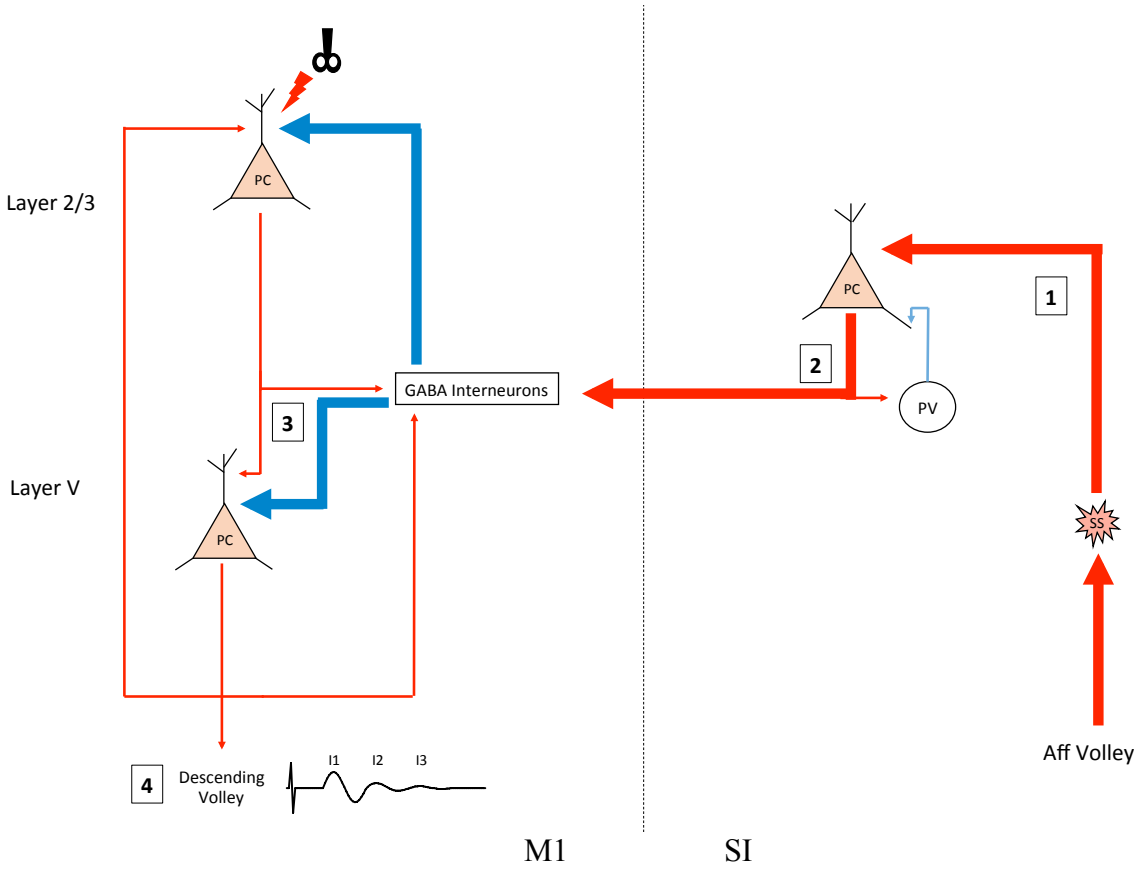

Figure 12: Mechanisms behind changes in MEPs and SAI due to spinal cord injury

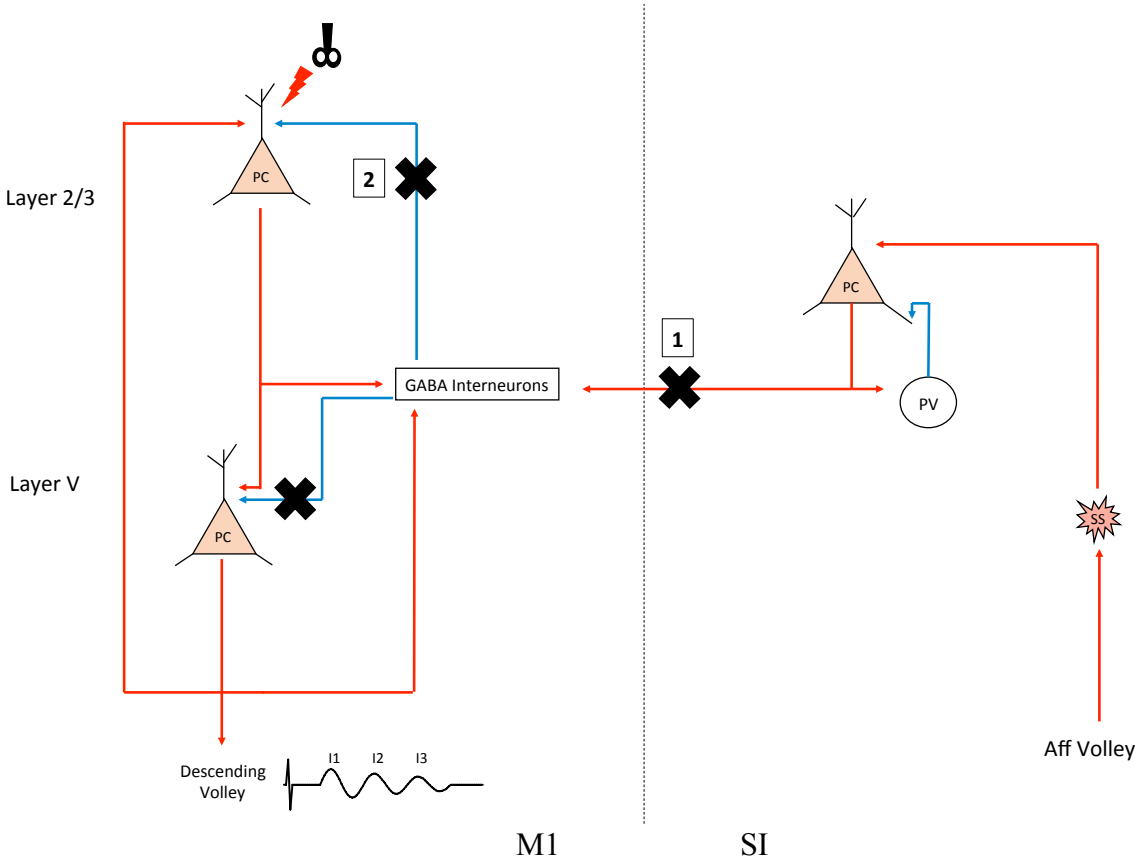

Figure Legends

Figure 9: Mechanisms in motor and somatosensory cortices

Figure 9 depicts the circuitries in somatosensory cortex and motor cortex mediating the generation of SEPs , PPR and SAI. 1. Depicts the arrival of the afferent volley into the somatosensory cortex by synapses from spiny stellate cells onto the pyramidal cells in layers IV/V, generating the SEP. 2. Depicts the generation of the PPR where the pyramidal cells synapse onto PV expressing inhibitor neurons that provide recurrent inhibition onto the pyramidal cell itself. 3. Depicts the generation of the MEP whereby the TMS pulse excites the pyramidal cells within layers II/III and V. These then create descending volleys that summate the spinal motor neurons and result in the muscle twitch. Cyclic excitation results in the period nature of the descending volleys.

Figure 10: Mechanisms behind short-latency afferent inhibition

Figure 10 depicts the mechanisms that mediate the generation of SAI. 1. The afferent volley arrives in the cortex and excites pyramidal cells. 2. Pyramidal cells have excitatory connections into motor cortex and are likely to be on GABAergic inhibitory neurons that modulate the descending volley. 3. The excitation from SI increases the inhibition from the GABAergic neurons that act on the pyramidal cells in M1. 4. The result is a decrease in the amplitude of the descending volleys specifically the late I-waves.

Figure 11: Mechanisms behind changing afferent intensity

Figure 11 depicts the mechanisms that mediate the changes that occur in measures of SEPs, PPR and SAI with increases in the afferent volley. 1. Increasing the afferent volley

increases the excitation within the pyramidal cells resulting in increased SEP. 2. The output from the pyramidal increases and increased excitation within M1 occurs but no increase in the excitation on the PV cells offering no increase in the amount of recurrent inhibition. 3. The increased excitation from SI increases the excitation onto the GABAergic neurons within M1. This increases the inhibitory output from these cells onto the pyramidal cells within M1. 4. The increase in inhibition onto the pyramidal cells will reduce the output and results in an increase in the inhibition in m1 and an increase in SAI.

Figure 12: Mechanisms behind changes in MEPs and SAI due to spinal cord injury

Figure 12 depicts the mechanisms that are altered in individuals with spinal cord injury. 1. Alterations in the excitatory synapses from SI to M1 may result in a reduction in the excitation of the GABAergic cells that would reduce the depth of SAI. 2. Intrinsic alterations in the GABAergic cells would reduce the ability to inhibit the pyramidal cells and would also reduce the depth of SAI.

5.3 Impact of experiments

Together these experiments provide new information regarding the function of motor cortex, somatosensory cortex and the interplay between the two in the upper limb in individuals with a cervical SCI in addition to detailing the relationship between afferent volley and measures indicating sensorimotor integration. Through the first experiment we have indicated several areas of neural function that are altered in individuals with SCI, and these areas may be targeted by plasticity inducing TMS protocols such as theta-burst stimulation and paired associated stimulation protocols to attempt to alter specific circuits. Restoring function to the altered neural circuits in this population could potentially result in functional gains, as proper neural function in both M1 and SI is essential for movement. However, there are limitations within our understanding of these measures that reduce the effectiveness of interpreting how well these protocols induce plasticity.

It is common for researchers to measure MEPs, SEPs and SAI before and after a plasticity protocol to test for its effectiveness on creating plasticity. To date several of these experiments have used measures of MT or multiples of MT to determine the stimulation protocol intensity [33-36]. The data in this thesis has shown that these intensities are actually at or above the saturation point for the measures of interest and disallows for increases caused by the stimulation protocol to be observed. I believe that in past literature there have been several stimulation protocols that have been "ineffective" at altering neural function but this conclusion may have been due to the intensity at which the measures of interest were evoked [36]. Therefore, it is important when designing

plasticity inducing research studies to ensure that the stimulation intensity is not above the individual's saturation point. This can be done by collecting an individual's recruitment curve prior to delivering the experimental protocol and setting the stimulation intensity to be on the sensitive part of the recruitment curve. If SEPs or SAI are the measure of interest we recommend that nerve stimulation intensities be based on measurements of SNAP since this is an objective method of determining stimulation intensity that is free of experimenter variability.

5.4 Limitations of Thesis

In Experiment 1 we measured of SEPs and SAI by stimulating the median nerve at 1.2 x MT. In our second experiment we show that 1.2 x MT corresponds to approximately 50% of the $SNAP_{max}$ and is also the point at which these measures saturate. If this information were available prior to designing Experiment 1 SNAP recruitment curves would have been collected in SCI similar to MEPs. This information would have provided an indication to how the cortex and peripheral nerves in an individual with SCI respond to a variation of stimulation intensities and would have possibly revealed differences in the saturation points between our two groups. It might be that SEPs in SCI are not normal, counter to our conclusions, and have an abnormal dose dependent response to increases in SNAPs something we did not test for. If this were the case it would alter our interpretation of the data in that cortical alterations in individuals with SCI leading to reduced SAI might be within SI and not in the transmission of afferents to M1 or within the M1 GABAergic neurons. It is important that we properly define where alterations exist in this population since stimulation protocols can be designed to affect the cortex

differently by altering location of stimulation, frequency of stimulation and/or the latency between paired associative stimulation protocols.

5.5 Conclusions

In summary the research contained in my thesis demonstrates that measures of motor function and sensorimotor integration are reduced in individuals with a cervical spinal cord injury. Specifically, MEPs are reduced and measures of SAI are reduced with nerve stimulation intensity is set to 1.2 x MT but measures of SEPs are not reduced. Further, the recruitment curves for SEPs and SAI show that there is an increase in both responses to an increase in the nerve stimulus and when stimulation intensity is determined by SNAPs these measures increase to 50% of $SNAP_{max}$ which is concurrent with 1.2 x MT. Additionally, SEPs and SAI are significantly correlated with SNAPs but SAI is not supporting the hypothesis that the afferent volley arrives in M1 via a relay through SI. Therefore, the reductions in MEPs seen in individuals with SCI are likely to be a result of damage to the descending efferent fibers while reductions in SAI are likely to be a result in either the transmission of the afferent volley to M1 from SI or within the GABAergic neurons within M1. Future research should develop stimulation protocols aimed at restoring proper function of these measures, which may lead to functional gains. This is important because individuals with cervical SCI have reported that restoring upper limb function is a top priority and the information collected in this thesis has provided a sound foundation to begin developing these protocols.

References

[1] Tokimura H, Di Lazzaro V, Tokimura Y, Oliviero A, Profice P, Insola A, et al. Short latency inhibition of human hand motor cortex by somatosensory input from the hand. J Physiol (Lond) 2000;523 Pt 2:503–13.

[2] Voller B, St Clair Gibson A, Lomarev M, Kanchana S, Dambrosia J, Dang N, et al. Long-latency afferent inhibition during selective finger movement. Journal of Neurophysiology 2005;94:1115–9. doi:10.1152/jn.00333.2005.

[3] Voller B, St Clair Gibson A, Dambrosia J, Pirio Richardson S, Lomarev M, Dang N, et al. Short-latency afferent inhibition during selective finger movement. Experimental Brain Research 2006;169:226–31. doi:10.1007/s00221-005-0140-9.

[4] Richardson SP, Bliem B, Lomarev M, Shamim E, Dang N, Hallett M. Changes in short afferent inhibition during phasic movement in focal dystonia. Muscle Nerve 2008;37:358–63. doi:10.1002/mus.20943.

[5] Kessler KR, Ruge D, Ilić TV, Ziemann U. Short latency afferent inhibition and facilitation in patients with writer's cramp. Mov Disord 2005;20:238–42. doi:10.1002/mds.20295.

[6] Sailer A, Molnar GF, Paradiso G, Gunraj CA, Lang AE, Chen R. Short and long latency afferent inhibition in Parkinson's disease. Brain 2003;126:1883–94. doi:10.1093/brain/awg183.

[7] Di Lazzaro V, Profice P, Pilato F, Capone F, Ranieri F, Florio L, et al. The level of cortical afferent inhibition in acute stroke correlates with long-term functional recovery in humans. Stroke 2012;43:250–2. doi:10.1161/STROKEAHA.111.631085.

[8] Nardone R, Bergmann J, Christova M, Caleri F, Tezzon F, Ladurner G, et al. Short latency afferent inhibition differs among the subtypes of mild cognitive impairment. J Neural Transm 2012;119:463–71. doi:10.1007/s00702-011-0725-3.

[9] Hu Y, Wen C-Y, Li T-H, Cheung MM-H, Wu EX-K, Luk KD-K. Somatosensory-evoked potentials as an indicator for the extent of ultrastructural damage of the spinal cord after chronic compressive injuries in a rat model. Clin Neurophysiol 2011;122:1440–7. doi:10.1016/j.clinph.2010.12.051.

[10] Edwards DJ, Cortes M, Thickbroom GW, Rykman A, Pascual-Leone A, Volpe BT. Preserved corticospinal conduction without voluntary movement after spinal cord injury. Spinal Cord 2013;51:765–7. doi:10.1038/sc.2013.74.

[11] Nardone R, Höller Y, Höller P, Thon N, Thomschewski A, Brigo F, et al. The role of the ipsilateral primary motor cortex in movement control after spinal cord injury: a TMS study. Neuroscience Letters 2013;552:21–4. doi:10.1016/j.neulet.2013.07.011.

[12] Kokotilo KJ, Eng JJ, Curt A. Reorganization and preservation of motor control of the brain in spinal cord injury: a systematic review. J Neurotrauma 2009;26:2113–26. doi:10.1089/neu.2008.0688.

[13] Raineteau O, Schwab ME. Plasticity of motor systems after incomplete spinal cord injury. Nat Rev Neurosci 2001;2:263–73. doi:10.1038/35067570.

[14] Collinger JL, Boninger ML, Bruns TM, Curley K, Wang W, Weber DJ. Functional priorities, assistive technology, and brain-computer interfaces after spinal cord injury. J Rehabil Res Dev 2013;50:145–60.
[15] Goshgarian HG. Spinal Cord Medicine: Principles and Practice. Demos Medical Publishing; 2010.
[16] Goshgarian HG. Chapter 1. In: Lin VW, editor. Spinal Cord Medicine: Principles and Practice, 2010.
[17] Kandel ER, Schwartz JH, Jessell TM. Principles of Neural Science. 4 ed. McGraw-Hill; 2000.
[18] Rowe M, Iwamura Y. Somatosensory Processing. CRC Press; 2003.
[19] Guillery RW, Feig SL, Lozsádi DA. Paying attention to the thalamic reticular nucleus. Trends Neurosci 1998;21:28–32.
[20] Dinse HR, Lillemeier A-S, Gatica Tossi MA, Tossi MAG. Influence of stimulation intensity on paired-pulse suppression of human median nerve somatosensory evoked potentials. NeuroReport 2013;24:451–6. doi:10.1097/WNR.0b013e3283616378.
[21] Neske GT, Patrick SL, Connors BW. Contributions of diverse excitatory and inhibitory neurons to recurrent network activity in cerebral cortex. J Neurosci 2015;35:1089–105. doi:10.1523/JNEUROSCI.2279-14.2015.
[22] Whitsel BL, Favorov O, Delemos KA, Lee C, Tommerdahl M, Essick GK, et al. SI neuron response variability is stimulus tuned and NMDA receptor dependent. Journal of Neurophysiology 1999;81:2988–3006.
[23] Lee CC, Imaizumi K. Functional convergence of thalamic and intrinsic projections to cortical layers 4 and 6. Neurophysiology 2013;45:396–406. doi:10.1007/s11062-013-9385-2.
[24] Gloor P. Neuronal generators and the problem of localization in electroencephalography: application of volume conductor theory to electroencephalography. Journal of Clinical Neurophysiology 1985;2:327–54.
[25] Iannella N, Tuckwell HC, Tanaka S. Firing properties of a stochastic PDE model of a rat sensory cortex layer 2/3 pyramidal cell. Math Biosci 2004;188:117–32. doi:10.1016/j.mbs.2003.10.002.
[26] Fischer M, Orth M. Short-latency sensory afferent inhibition: conditioning stimulus intensity, recording site, and effects of 1 Hz repetitive TMS. Brain Stimulation 2011;4:202–9. doi:10.1016/j.brs.2010.10.005.
[27] Asmussen MJ, Zapallow CM, Jacobs MF, Lee KGH, Tsang P, Nelson AJ. Modulation of short-latency afferent inhibition depends on digit and task-relevance. PLoS ONE 2014;9:e104807. doi:10.1371/journal.pone.0104807.
[28] Asmussen MJ, Jacobs MF, Lee KGH, Zapallow CM, Nelson AJ. Short-latency afferent inhibition modulation during finger movement. PLoS ONE 2013;8:e60496. doi:10.1371/journal.pone.0060496.
[29] Short latency inhibition of human hand motor cortex by somatosensory input from the hand. 2000;523 Pt 2:503–13.
[30] Oliviero A, Ranieri F, Pilato F, Dileone M, Capone F, Di Lazzaro V, et al. I-wave origin and modulation. Brain Stimulation 2012;5:512–25. doi:10.1016/j.brs.2011.07.008.

[31] Petrof I, Viaene AN, Sherman SM. Properties of the primary somatosensory cortex projection to the primary motor cortex in the mouse. Journal of Neurophysiology 2015;113:2400–7. doi:10.1152/jn.00949.2014.
[32] Sherman SM. Thalamocortical interactions. Curr Opin Neurobiol 2012;22:575–9. doi:10.1016/j.conb.2012.03.005.
[33] Quartarone A, Rizzo V, Bagnato S, Morgante F, Sant'Angelo A, Girlanda P, et al. Rapid-rate paired associative stimulation of the median nerve and motor cortex can produce long-lasting changes in motor cortical excitability in humans. J Physiol (Lond) 2006;575:657–70. doi:10.1113/jphysiol.2006.114025.
[34] Tsang P, Jacobs MF, Lee KGH, Asmussen MJ, Zapallow CM, Nelson AJ. Continuous theta-burst stimulation over primary somatosensory cortex modulates short-latency afferent inhibition. Clin Neurophysiol 2014. doi:10.1016/j.clinph.2014.02.026.
[35] Tsang P, Bailey AZ, Nelson AJ. Rapid-rate paired associative stimulation over the primary somatosensory cortex. PLoS ONE 2015;10:e0120731. doi:10.1371/journal.pone.0120731.
[36] Kriváneková L, Lu M-K, Bliem B, Ziemann U. Modulation of excitability in human primary somatosensory and motor cortex by paired associative stimulation targeting the primary somatosensory cortex. Eur J Neurosci 2011;34:1292–300. doi:10.1111/j.1460-9568.2011.07849.x.
[37] Wolters A, Wolters A, Sandbrink F, Schlottmann A, Kunesch E, Stefan K, et al. A Temporally Asymmetric Hebbian Rule Governing Plasticity in the Human Motor Cortex. Journal of Neurophysiology 2003;89:2339–45. doi:10.1152/jn.00900.2002.
[38] Lesser RP, Koehle R, Lueders H. Effect of stimulus intensity on short latency somatosensory evoked potentials. Electroencephalogr Clin Neurophysiol 1979;47:377–82.
[39] Mountcastle VB. The Sensory Hand. 1st ed. Harvard University Press; 2006.
[40] Felleman DJ, Nelson RJ, Sur M, Kaas JH. Representations of the body surface in areas 3b and 1 of postcentral parietal cortex of Cebus monkeys. Brain Research 1983;268:15–26.
[41] Felleman DJ, Wall JT, Cusick CG, Kaas JH. The representation of the body surface in S-I of cats. Journal of Neuroscience 1983;3:1648–69.
[42] Nelson RJ. The Somatosensory System. CRC Press; 2001.
[43] Goff GD, Matsumiya Y, Allison T, Goff WR. The scalp topography of human somatosensory and auditory evoked potentials. Electroencephalogr Clin Neurophysiol 1977;42:57–76.
[44] Allison T, Wood CC, Goff WR. Brain stem auditory, pattern-reversal visual, and short-latency somatosensory evoked potentials: latencies in relation to age, sex, and brain and body size. Electroencephalogr Clin Neurophysiol 1983;55:619–36.
[45] Allison T, McCarthy G, Wood CC. The relationship between human long-latency somatosensory evoked potentials recorded from the cortical surface and from the scalp. Electroencephalogr Clin Neurophysiol 1992;84:301–14.

[46] Gandevia SC, Burke D. Saturation in human somatosensory pathways. Experimental Brain Research 1984;54:582–5.
[47] Ugawa Y, Genba-Shimizu K, Kanazawa I. Somatosensory evoked potential recovery (SEP-R) in various neurological disorders. Electroencephalogr Clin Neurophysiol 1996;100:62–7.
[48] Vogt BA, Pandya DN. Cortico-cortical connections of somatic sensory cortex (areas 3, 1 and 2) in the rhesus monkey. J Comp Neurol 1978;177:179–91. doi:10.1002/cne.901770202.
[49] Chung S, Li X, Nelson SB. Short-term depression at thalamocortical synapses contributes to rapid adaptation of cortical sensory responses in vivo. Neuron 2002;34:437–46.
[50] Petersen CCH. Short-term dynamics of synaptic transmission within the excitatory neuronal network of rat layer 4 barrel cortex. Journal of Neurophysiology 2002;87:2904–14.
[51] Cruikshank SJ, Lewis TJ, Connors BW. Synaptic basis for intense thalamocortical activation of feedforward inhibitory cells in neocortex. Nat Neurosci 2007;10:462–8. doi:10.1038/nn1861.
[52] Jones EG, Powell TP. Connexions of the somatic sensory cortex of the rhesus monkey. I. Ipsilateral cortical connexions. Brain 1969;92:477–502.
[53] Pandya DN, Kuypers HG. Cortico-cortical connections in the rhesus monkey. Brain Research 1969;13:13–36.
[54] Pavlides C, Miyashita E, Asanuma H. Projection from the sensory to the motor cortex is important in learning motor skills in the monkey. Journal of Neurophysiology 1993;70:733–41.
[55] Terao Y, Ugawa Y. Basic mechanisms of TMS. Journal of Clinical Neurophysiology 2002;19:322–43.
[56] Hallett M. Transcranial magnetic stimulation: a primer. Neuron 2007;55:187–99. doi:10.1016/j.neuron.2007.06.026.
[57] Rossi S, Hallett M, Rossini PM, Pascual-leone A, Safety of TMS Consensus Group. Safety, ethical considerations, and application guidelines for the use of transcranial magnetic stimulation in clinical practice and research. Clin Neurophysiol, vol. 120, 2009, pp. 2008–39. doi:10.1016/j.clinph.2009.08.016.
[58] Siebner HR, Rothwell J. Transcranial magnetic stimulation: new insights into representational cortical plasticity. Experimental Brain Research 2003;148:1–16. doi:10.1007/s00221-002-1234-2.
[59] Rossini PM, Rossi S. Transcranial magnetic stimulation: diagnostic, therapeutic, and research potential. Neurology 2007;68:484–8. doi:10.1212/01.wnl.0000250268.13789.b2.
[60] Rothwell JC. Using transcranial magnetic stimulation methods to probe connectivity between motor areas of the brain. Hum Mov Sci 2011;30:906–15. doi:10.1016/j.humov.2010.07.007.
[61] Petersen NT, Pyndt HS, Nielsen JB. Investigating human motor control by transcranial magnetic stimulation. Experimental Brain Research 2003;152:1–16. doi:10.1007/s00221-003-1537-y.
[62] Paulus W, Classen J, Cohen LG, Large CH, Di Lazzaro V, Nitsche M, et al.

State of the art: Pharmacologic effects on cortical excitability measures tested by transcranial magnetic stimulation. Brain Stimulation 2008;1:151–63. doi:10.1016/j.brs.2008.06.002.

[63] Ziemann U, Rossini PM, Thickbroom GW, Kaelin-Lang A, Mima T, Groppa S, et al. A practical guide to diagnostic transcranial magnetic stimulation: Report of an IFCN committee. Clinical Neurophysiology 2012;123:858–82. doi:10.1016/j.clinph.2012.01.010.

[64] Rossini PM, Barker AT, Berardelli A, Caramia MD, Caruso G, Cracco RQ, et al. Non-invasive electrical and magnetic stimulation of the brain, spinal cord and roots: basic principles and procedures for routine clinical application. Report of an IFCN committee. Electroencephalogr Clin Neurophysiol 1994;91:79–92.

[65] Ziemann U. TMS induced plasticity in human cortex. Rev Neurosci 2004;15:253–66.

[66] Hirashima F, Yokota T. Influence of peripheral nerve stimulation on human motor cortical excitability in patients with ventrolateral thalamic lesion. Arch Neurol 1997;54:619–24.

[67] Chen R, Corwell B, Hallett M. Modulation of motor cortex excitability by median nerve and digit stimulation. Experimental Brain Research 1999;129:77–86.

[68] Tamburin S, Manganotti P, Zanette G, Fiaschi A, Tamburin S, Manganotti P, et al. Cutaneomotor integration in human hand motor areas: somatotopic effect and interaction of afferents. Experimental Brain Research 2001;141:232–41. doi:10.1007/s002210100859.

[69] Classen J, Steinfelder B, Liepert J, Stefan K, Celnik P, Cohen LG, et al. Cutaneomotor integration in humans is somatotopically organized at various levels of the nervous system and is task dependent. Experimental Brain Research 2000;130:48–59.

[70] Reis J, Swayne OB, Vandermeeren Y, Camus M, Dimyan MA, Harris-Love M, et al. Contribution of transcranial magnetic stimulation to the understanding of cortical mechanisms involved in motor control. J Physiol (Lond) 2008;586:325–51. doi:10.1113/jphysiol.2007.144824.

[71] Di Lazzaro V, Oliviero A, Profice P, Pennisi MA, Di Giovanni S, Zito G, et al. Muscarinic receptor blockade has differential effects on the excitability of intracortical circuits in the human motor cortex. Experimental Brain Research 2000;135:455–61.

[72] Di Lazzaro V, Oliviero A, Pilato F, Saturno E, Dileone M, Marra C, et al. Motor cortex hyperexcitability to transcranial magnetic stimulation in Alzheimer's disease. J Neurol Neurosurg Psychiatr 2004;75:555–9.

[73] Di Lazzaro V, Pilato F, Dileone M, Tonali PA, Ziemann U. Dissociated effects of diazepam and lorazepam on short-latency afferent inhibition. J Physiol (Lond) 2005;569:315–23. doi:10.1113/jphysiol.2005.092155.

[74] Bertolasi L, Priori A, Tinazzi M, Bertasi V, Rothwell JC. Inhibitory action of forearm flexor muscle afferents on corticospinal outputs to antagonist muscles in humans. J Physiol (Lond) 1998;511 (Pt 3):947–56.

[75] Bäumer T, Helmich RCG, Bloem BR, Siebner HR, Münchau A. Hemispheric

asymmetry and somatotopy of afferent inhibition in healthy humans. Experimental Brain Research 2005;167:211–9. doi:10.1007/s00221-005-0014-1.

[76] Kim RC. Chapter 2. In: Lin VW, editor. Spinal Cord Medicine: Principles and Practice, Demos Medical Publishing; 2010.

[77] Lee RR, Hart BL. Chapter 3. In: Lin VW, editor. Spinal Cord Medicine: Principles and Practice, Demos Medical Publishing; 2010.

[78] Marino RJ. Chapter 5. In: Lin VW, editor. Spinal Cord Medicine: Principles and Practice, Demos Medical Publishing; 2010.

[79] Buonomano DV, Merzenich MM, Buonomano DV, Merzenich MM. CORTICAL PLASTICITY: From Synapses to Maps. Annu Rev Neurosci 1998;21:149–86. doi:10.1146/annurev.neuro.21.1.149.

[80] Bütefisch CM, Davis BC, Wise SP, Sawaki L, Kopylev L, Classen J, et al. Mechanisms of use-dependent plasticity in the human motor cortex. Proc Natl Acad Sci USa 2000;97:3661–5. doi:10.1073/pnas.050350297.

[81] Norton JA, Gorassini MA, Norton JA. Changes in Cortically Related Intermuscular Coherence Accompanying Improvements in Locomotor Skills in Incomplete Spinal Cord Injury. Journal of Neurophysiology 2005;95:2580–9. doi:10.1152/jn.01289.2005.

[82] Knikou M. The H-reflex as a probe: pathways and pitfalls. J Neurosci Methods 2008;171:1–12. doi:10.1016/j.jneumeth.2008.02.012.

[83] Shields RK, Dudley-Javoroski S, Oza PD. Low-frequency H-reflex depression in trained human soleus after spinal cord injury. Neuroscience Letters 2011;499:88–92. doi:10.1016/j.neulet.2011.05.040.

[84] Freund P, Thompson AJ, Rothwell J, Craggs M, Bestmann S. Corticomotor representation to a human forearm muscle changes following cervical spinal cord injury. The European Journal of Neuroscience 2011;34:1839–46. doi:10.1111/j.1460-9568.2011.07895.x.

[85] Saturno E, Bonato C, Miniussi C, Lazzaro V, Callea L. Motor cortex changes in spinal cord injury: a TMS study. Neurol Res 2008;30:1084–5. doi:10.1179/174313208X332968.

[86] Roy FD, Yang JF, Gorassini MA, Roy FD, Yang JF, Gorassini MA. Afferent Regulation of Leg Motor Cortex Excitability After Incomplete Spinal Cord Injury. Journal of Neurophysiology 2010;103:2222–33. doi:10.1152/jn.00903.2009.

[87] Mikulis DJ, Jurkiewicz MT, McIlroy WE, Staines WR, Rickards L, Kalsi-Ryan S, et al. Adaptation in the motor cortex following cervical spinal cord injury. Neurology 2002;58:794–801.

[88] Jurkiewicz MT, Crawley AP, Verrier MC, Fehlings MG, Mikulis DJ. Somatosensory cortical atrophy after spinal cord injury: a voxel-based morphometry study. Neurology 2006;66:762–4. doi:10.1212/01.wnl.0000201276.28141.40.

[89] Roy FD, Zewdie ET, Gorassini MA. Short-interval intracortical inhibition with incomplete spinal cord injury. Clin Neurophysiol 2011;122:1387–95. doi:10.1016/j.clinph.2010.11.020.

[90] Davey NJ, Smith HC, Savic G, Maskill DW, Ellaway PH, Frankel HL.

Comparison of input-output patterns in the corticospinal system of normal subjects and incomplete spinal cord injured patients. Experimental Brain Research 1999;127:382–90.

[91] Ni Z, Charab S, Gunraj C, Nelson AJ, Udupa K, Yeh I-J, et al. Transcranial magnetic stimulation in different current directions activates separate cortical circuits. Journal of Neurophysiology 2011;105:749–56. doi:10.1152/jn.00640.2010.

[92] Jurkiewicz MT, Mikulis DJ, McIlroy WE, Fehlings MG, Verrier MC. Sensorimotor cortical plasticity during recovery following spinal cord injury: a longitudinal fMRI study. Neurorehabilitation and Neural Repair 2007;21:527–38. doi:10.1177/1545968307301872.

[93] Gott PS, Karnaze DS, Fisher M. Assessment of median nerve somatosensory evoked potentials in cerebral ischemia. Stroke 1990;21:1167–71.

[94] Hodgkin AL, Huxley AF. A quantitative description of membrane current and its application to conduction and excitation in nerve. 1952. vol. 52. 1990.

[95] Ziemann U, Lönnecker S, Steinhoff BJ, Paulus W. Effects of antiepileptic drugs on motor cortex excitability in humans: a transcranial magnetic stimulation study. Ann Neurol 1996;40:367–78. doi:10.1002/ana.410400306.

[96] Kimiskidis VK, Papagiannopoulos S, Sotirakoglou K, Kazis DA, Kazis A, Mills KR. Silent period to transcranial magnetic stimulation: construction and properties of stimulus-response curves in healthy volunteers. Experimental Brain Research 2005;163:21–31. doi:10.1007/s00221-004-2134-4.

[97] Mavroudakis N, Caroyer JM, Brunko E, Zegers de Beyl D. Effects of diphenylhydantoin on motor potentials evoked with magnetic stimulation. Electroencephalogr Clin Neurophysiol 1994;93:428–33.

[98] Chen R, Samii A, Caños M, Wassermann EM, Hallett M. Effects of phenytoin on cortical excitability in humans. Neurology 1997;49:881–3.

[99] Boroojerdi B, Battaglia F, Muellbacher W, Cohen LG. Mechanisms influencing stimulus-response properties of the human corticospinal system. Clin Neurophysiol 2001;112:931–7.

[100] Schönle PW, Isenberg C, Crozier TA, Dressler D, Machetanz J, Conrad B. Changes of transcranially evoked motor responses in man by midazolam, a short acting benzodiazepine. Neuroscience Letters 1989;101:321–4.

[101] Ilić TV, Meintzschel F, Cleff U, Ruge D, Kessler KR, Ziemann U. Short-interval paired-pulse inhibition and facilitation of human motor cortex: the dimension of stimulus intensity. J Physiol (Lond) 2002;545:153–67.

[102] Kimiskidis VK, Papagiannopoulos S, Kazis DA, Sotirakoglou K, Vasiliadis G, Zara F, et al. Lorazepam-induced effects on silent period and corticomotor excitability. Experimental Brain Research 2006;173:603–11. doi:10.1007/s00221-006-0402-1.

[103] Mohammadi B, Krampfl K, Petri S, Bogdanova D, Kossev A, Bufler J, et al. Selective and nonselective benzodiazepine agonists have different effects on motor cortex excitability. Muscle Nerve 2006;33:778–84.

doi:10.1002/mus.20531.
[104] Inghilleri M, Berardelli A, Marchetti P, Manfredi M. Effects of diazepam, baclofen and thiopental on the silent period evoked by transcranial magnetic stimulation in humans. Experimental Brain Research 1996;109:467–72.
[105] Di Lazzaro V, Oliviero A, Tonali PA, Marra C, Daniele A, Profice P, et al. Noninvasive in vivo assessment of cholinergic cortical circuits in AD using transcranial magnetic stimulation. Neurology 2002;59:392–7.
[106] Di Lazzaro V, Oliviero A, Pilato F, Saturno E, Dileone M, Marra C, et al. Neurophysiological predictors of long term response to AChE inhibitors in AD patients. J Neurol Neurosurg Psychiatr 2005;76:1064–9. doi:10.1136/jnnp.2004.051334.
[107] Nashed J, Calder K, Trachter R, McLean L. The consequences of stimulus intensity on sensory nerve action potentials. J Neurosci Methods 2009;185:108–15. doi:10.1016/j.jneumeth.2009.09.018.
[108] Lin Y-Y, Shih Y-H, Chen J-T, Hsieh J-C, Yeh T-C, Liao K-K, et al. Differential effects of stimulus intensity on peripheral and neuromagnetic cortical responses to median nerve stimulation. NeuroImage 2003;20:909–17. doi:10.1016/S1053-8119(03)00387-2.
[109] Oldfield RC. The assessment and analysis of handedness: the Edinburgh inventory. Neuropsychologia 1971;9:97–113.
[110] Höffken O, Veit M, Knossalla F, Lissek S, Bliem B, Ragert P, et al. Sustained increase of somatosensory cortex excitability by tactile coactivation studied by paired median nerve stimulation in humans correlates with perceptual gain. J Physiol (Lond) 2007;584:463–71. doi:10.1113/jphysiol.2007.140079.
[111] Allison T. Recovery functions of somatosensory evoked responses in man. Electroencephalogr Clin Neurophysiol 1962;14:331–43.
[112] McLaughlin DF, Kelly EF. Evoked potentials as indices of adaptation in the somatosensory system in humans: a review and prospectus. Brain Res Brain Res Rev 1993;18:151–206.
[113] Allison T, McCarthy G, Wood CC, Jones SJ. Potentials evoked in human and monkey cerebral cortex by stimulation of the median nerve. A review of scalp and intracranial recordings. Brain 1991;114 (Pt 6):2465–503.
[114] Backes WH, Mess WH, van Kranen-Mastenbroek V, Reulen JP. Somatosensory cortex responses to median nerve stimulation: fMRI effects of current amplitude and selective attention. Clin Neurophysiol 2000;111:1738–44.
[115] Nelson AJ, Staines WR, Graham SJ, McIlroy WE. Activation in SI and SII: the influence of vibrotactile amplitude during passive and task-relevant stimulation. Brain Res Cogn Brain Res 2004;19:174–84. doi:10.1016/j.cogbrainres.2003.11.013.
[116] Simons SB, Tannan V, Chiu J, Favorov OV, Whitsel BL, Tommerdahl M. Amplitude-dependency of response of SI cortex to flutter stimulation. BMC Neurosci 2005;6:43. doi:10.1186/1471-2202-6-43.
[117] Chen LM, Friedman RM, Roe AW. Optical imaging of a tactile illusion in

area 3b of the primary somatosensory cortex. Science 2003;302:881–5. doi:10.1126/science.1087846.

[118] Arthurs OJ, Williams EJ, Carpenter TA, Pickard JD, Boniface SJ. Linear coupling between functional magnetic resonance imaging and evoked potential amplitude in human somatosensory cortex. Neuroscience 2000;101:803–6.

[119] Nardone R, Höller Y, Bathke AC, Orioli A, Schwenker K, Frey V, et al. Spinal cord injury affects I-wave facilitation in human motor cortex. Brain Research Bulletin 2015;116:93–7. doi:10.1016/j.brainresbull.2015.06.006.

[120] Cirillo J, Calabro FJ, Perez MA. Impaired Organization of Paired-Pulse TMS-Induced I-Waves After Human Spinal Cord Injury. Cereb Cortex 2015:bhv048. doi:10.1093/cercor/bhv048.